Department of Mathematics and Statistics

Optimal control of diabetes

Zahra Hassan A Al Helal

This thesis is presented for the Degree of
Doctor of Philosophy
of
Curtin University

May 2016

Declaration

I affirm that the material in this thesis is the result of my own original research and has not been submitted for any other degree, diploma, or award.

.....
Zahra Hassan A Al Helal
May 2016

Dedication

This thesis is dedicated to my dear husband, Haider, who has been a constant source of support and encouragement during the challenges which I have been through until the completion of this thesis. My PhD studies seemed like climbing a high mountain step by step and the journey was made possible with his encouragement, sacrifices and trust.

Zahra

Abstract

In this thesis, we are concerned with optimal control problems related to one of the major global health problems facing human beings, diabetes, with a staggering 4.9 million deaths attributed to it in 2014. Diabetes is an incurable disease caused when the pancreas no longer makes insulin (in the case of type 1 diabetes), or when the pancreas cannot make enough insulin and/or the body develops insulin resistance (in the case of type 2 diabetes). The ultimate aim of this thesis is to propose and illustrate a general methodology for the analysis and control of the human blood glucose regulatory system.

We adopt a comprehensive dynamic model of the blood glucose regulatory system and show how it can be readily fitted to individuals. This is done by formulating an optimal parameter selection problem in which optimal values for the model parameters must be selected so that the resulting model best fits the desired data. Then, a numerical solution procedure for this optimal parameter selection problem using the optimal control software MISER3.3 is proposed. We also investigate the sensitivity of the resulting optimized model with respect to the insulin release rate, which is the body's natural feedback control. Moreover, we demonstrate how optimal open loop controls can be readily calculated for this model.

We then extend the model to include bolus insulin injections for the treatment of diabetic patients. We also show how to incorporate the role of exercise into this model. We formulate the combined model as an optimal control problem in which the aim is to determine optimal injection times, optimal injection volumes and optimal exercise regimes to regulate the blood glucose level. A numerical approach, based on control parameterization and a time scaling transformation, is then developed for solving the optimal control problem. Numerical results for different scenarios involving type 1 and type 2 diabetes show that optimal treatment regimes can be readily determined via the proposed approach. The optimal regimes are successful at regulating the blood glucose level.

In future work, improvements can be made to incorporate other important treatment regimes, particularly for type 2 diabetics, into the model.

List of publications

The following paper (which has been published) was completed during PhD candidature:

- Z. Al Helal, V. Rehbock, and R. C. Loxton, "Modeling and Optimal Control of Blood Glucose Levels in the Human Body," *Journal of Industrial and Management Optimization*, vol. 11, no. 4, pp. 1149-1164, 2015.

The following paper was completed during PhD candidature and will be submitted soon:

- Z. Al Helal, V. Rehbock, and R. C. Loxton, " Insulin Injections and Exercise Scheduling for Diabetics: an Optimal Control Model"

Acknowledgements

The research reported in this thesis was carried out between February 2012 and May 2016, while I was a PhD student in the Department of Mathematics and Statistics, Curtin University. I am very grateful for the help I received from friends, family, teachers, and colleagues during this time. Without it, this thesis could not be completed.

I am especially indebted to my supervisors, A/Prof. Volker Rehbock and A/Prof. Ryan Loxton. They have guided my research during the past four years with remarkable patience and enthusiasm. A/Prof. Rehbock, in particular, should be commended for persevering with me for so long: he was also the supervisor of my master degree project on the optimal control of chemical processes. A/Prof. Loxton, meanwhile, deserves special thanks for encouraging me to attend conferences in Taiwan and Canberra.

I thank all of the staff in the Department of Mathematics and Statistics for contributing to a friendly work environment. I am also particularly grateful to Mr Peter Mckinnon, as he was the lecturer-in-charge of the courses that I taught as a sessional tutor.

I have really enjoyed working with the other students in the Department of Mathematics and Statistics, especially Samira Shaban Albrbar, Dewi Tjia. I thank each of them for being a wonderful friend and colleague.

Finally, on a more personal note, I sincerely thank everyone in my family, particularly my husband, for his support and encouragement during my PhD candidature.

List of Figures

List of Tables

Contents

CHAPTER 1

Introduction

1.1 Blood glucose regulatory system

In this thesis, we are concerned with optimal control problems related to human health. One of the major global health problems is diabetes with a staggering 4.9 million deaths attributed to it in 2014 [2]. Figures about diabetes released by the International Diabetes Federation (IDF) show that 387 million people worldwide have diabetes. The Western Pacific region, which includes highly developed countries such as Australia and Japan, and fast growing economies such as China, accounts for 138 million diabetes sufferers [2].

Correct blood glucose levels are crucial to maintaining health. The normal concentration of blood glucose in a healthy person is between 80 to 120 mg/dl (4.4 to 6.7 mmol/l). Concentrations outside of this range cause either hyperglycemia (above 120 mg/dl) or hypoglycemia (under 80 mg/dl). Prolonged irregularities in the blood glucose level result in major health problems.

Diabetes is an incurable disease caused when the pancreas no longer makes insulin (in the case of type 1 diabetes), or when the pancreas cannot make enough insulin and/or the body develops insulin resistance (in the case of type 2 diabetes). Some common signs and symptoms of diabetes are increased thirst, frequent urination, extreme hunger, fatigue, blurred vision, slow-healing sores and the presence of ketones in the urine (ketones are the byproducts of broken down fatty acids in the body that increase due to weight loss or when there is not enough insulin available). Left unmanaged, diabetes has harmful effects on the vascular system due to the resulting high blood glucose levels [19]. Macrovascular complications are driven by atherosclerosis (the formation of fibrofatty plaque on artery walls) which leads to the narrowing of arterial walls throughout the body and can result in strokes or cardiac arrest. Microvascular complications are due to damage to very small blood vessels and nerves. Diabetic retinopathy results from damage to the tiny blood vessels at the back of the eye and can seriously affect vision to the point of blindness. Diabetic nephropathy is a similar process occurring in the kidneys which reduces their ability to filter blood properly and may lead to complete kidney failure. Finally, diabetic

neuropathy is the dysfunction of peripheral nerves which results in the inability to feel pain in the extremities of the body, particularly in the hands and feet. This frequently results in undetected injuries which do not heal well and may require amputations. Hypoglycemia, on the other hand, causes serious short term impacts such as fainting, brain failure and death. In addition to type 1 and type 2 diabetes, there are other forms of diabetes such as gestational diabetes which may occur during pregnancy and often disappears after the birth of the child.

Before going deeper into the blood glucose regulatory system, it is worth giving a description of the main components. Glucose is the simplest form of sugar and represents the primary source of energy for cells in the human body. Glycogen has a modified molecular structure compared to glucose and is generated for the purpose of storing energy in the body. Insulin is a natural hormone made by the pancreas which regulates the blood glucose level. Cells cannot absorb glucose directly from the bloodstream without insulin. Glucagon, a natural hormone made by alpha cells in the pancreas, promotes the glycogenolysis process (the breakdown of glycogen to glucose) in the liver.

In a healthy person, stabilization of the blood glucose level in the normal range is achieved in multiple ways. The hormones insulin, which is produced by β cells, and glucagon, which is produced by α cells, are the most important regulators of the blood glucose level. They are both secreted by the endocrine pancreas and stabilize the glucose level in the blood via natural feedback loops. When the glucose concentration rises too high, insulin is secreted which encourages glucose uptake by cells as well as conversion of glucose to glycogen, there by lowering the blood glucose concentration. In the opposite manner, a decrease in blood glucose below the desired level stimulates glucagon secretion which in turn increases the glucose concentration towards normal through the conversion of glycogen to glucose. Factors affecting the blood glucose concentration can be divided into five categories:

(i) Food intake. This includes the timing of meals, composition of the food and quantity.

(ii) Medication used in the case of a diabetic subject. This includes insulin and other drugs which stimulate insulin production or reduce insulin resistance in the body.

(iii) The level of exercise of an individual.

(iv) Biological factors such as stress or illness.

(v) Environmental factors such as climate and altitude.

For diabetic patients in particular, additional factors can have a significant impact on blood glucose levels:

(i) The type of insulin preparation used (short or long acting).

Types of insulin	Action	Example
fast or rapid-acting insulin	onset within 15 mins. after injection, reaches peak between 30 to 90 mins. and lasts for 3 to 5 hrs.	insulin aspart and insulin lispro
short-acting insulin	onset within 30 to 60 mins. after injection, reaches peak between 2 to 4 hrs. and lasts for 5 to 8 hrs.	regular
intermediate-acting insulin	onset within 1 to 3 hrs. after injection, reaches peak after 8 hrs. and lasts for 12 to 16 hrs.	NPH
long-acting insulin	onset within 1 hour of injection, is peak-less and lasts for 20 to 26 hrs (1 or 2 injections last for a whole day)	insulin glargine
mixed insulin	Is a combination of either rapid-acting or short acting insulin with an intermediate-acting insulin, onset within 10 to 15 mins, its peak varies and lasts for 10 to 16 hrs.	75% insulin lispro protamine and 25% insulin lispro, 70% insulin aspart protamine and 30% insulin aspart, or regular with NPH

Table 1.1: Insulin types and their characteristics (onset, peak times and duration)

(ii) The injection site and delivery type (bolus or continuous infusion).

(iii) The patient's characteristics.

Since physical characteristics vary from person to person, different patients usually have somewhat different responses to the same treatment. Even responses of the same patient to the same treatment can vary under different circumstances.

For each type of insulin, there is an onset time (i.e. when the insulin starts to work after it is taken), a peak time (i.e. when the maximum effect of insulin is observed) and a duration (i.e. the time during which the insulin continues to work). These characteristics vary amongst insulin types and they may also differ from patient to patient. Table 1.1 gives a brief overview of insulin types and their estimated characteristics (onset, peak times and duration).

To survive type 1 diabetes, a lifetime of exogenous insulin injections and regular monitoring of blood glucose concentration is required. On the other hand, type 2 diabetics

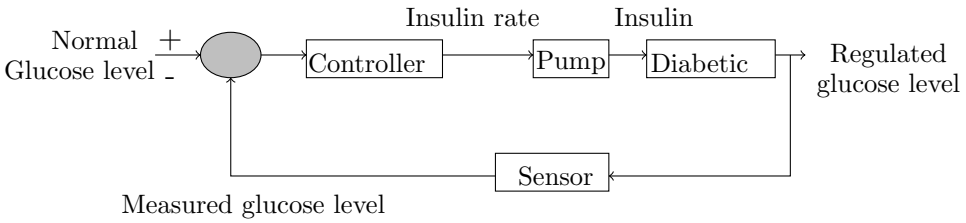

Figure 1.1: Closed loop system

require insulin only when diet restrictions, increased physical activity and non insulin medications are insufficient to control blood glucose levels. Therefore, the problem of closed loop blood glucose level regulation via insulin infusion has been the subject of investigations for decades, with studies conducted in both an empirical framework and a mathematical one. While the empirical framework involves clinical experience and knowledge, the mathematical framework uses mathematical models (which describe the intrinsic glucose regulation performed by the endocrine pancreas) to formulate appropriate schemes for regulation of the blood glucose level.

The formulation of a control rule is based on the knowledge we have about components of the closed loop system which is often referred to as an artificial pancreas (see Figure 1.1). Thus, the ultimate aim of a control algorithm is to mimic the functionality of the pancreas . While these control algorithms are usually closed loop in practice, their design can be enhanced significantly by comparison to corresponding open loop optimal controls. One aim of this thesis is to construct open loop optimal controls for diabetic patients.

Mathematically based control methods rely on dynamical models of the body's blood glucose regulatory system. To date, several nonlinear mathematical models for the blood glucose regulatory system have been proposed. These range from simple ones such as the Bergman minimal model [10], which has been widely cited, to more comprehensive ones [13]. Comprehensive models aim to integrate knowledge about the blood glucose regulation system into a large nonlinear compartmental model involving a variety of parameters and factors that influence the system. Several control models, such as proportional-integral-derivative (PID) control [38], robust servo control [28], and model predictive control (MPC) [23], have been developed based on the Bergman minimal model. In most of the existing control models, the glucose regulatory system is greatly simplified and only glucose and insulin are considered. We will discuss a variety of dynamic and control models in more detail in the next chapter of this thesis.

The aim of this thesis is to propose and illustrate a general methodology for the analysis and control of the human blood glucose regulatory system. We adopt a comprehensive dynamic model of intermediate complexity and show how it can be readily fitted to

individuals. We also demonstrate how optimal open loop controls can be calculated for this model. We then extend the model to include bolus insulin injections for the treatment of diabetic patients. We also show how to incorporate the role of exercise into this model and determine combined optimal insulin delivery and exercise regimes. Finally, we point out other important treatment regimes that should also be incorporated into the model in the future.

1.2 Optimal control

Optimal control and optimal parameter selection problems arise in many fields such as financial management, forestry, agriculture, defense, civil, chemical, electrical and mechanical engineering, biology and the social sciences. Broadly speaking, an optimal control problem seeks to optimize a performance index subject to a set of dynamic and, possibly, algebraic constraints. The dynamic constraints may consist of a set of differentiable equations (ordinary or partial) or a set of difference equations. These equations may be deterministic or stochastic in nature. In this thesis, we formulate and solve several practical problems related to the insulin-glucose dynamics in the human body. These formulations are in the form of optimal parameter selection problems as well as combined optimal parameter selection and optimal control problems involving systems of ordinary differential equations. We give a general formulation of these problems and discuss their solution methods in this and the following sections.

A general formulation of a basic optimal control problem can be described as follows. Consider the dynamical system

$$\dot{x}(t) = f(t, x(t), u(t)), \tag{1.1}$$

over the time horizon $t \in [0, T]$ and the initial condition

$$x(0) = x^0, \tag{1.2}$$

where

- $x(t) \in \mathbb{R}^n$ is the state vector at time t;
- $u(t) \in \mathbb{R}^r$ is the control vector (whose components are the control variables) at time t;
- $f : \mathbb{R} \times \mathbb{R}^n \times \mathbb{R}^r \to \mathbb{R}^n$ is a given function, assumed to be continuously differentiable with respect to x and u, and piecewise continuous with respect to time t;
- T is the terminal time;

- $x^0 \in \mathbb{R}^n$ is a given initial state vector;
- n is the number of states; and
- r is the number of controls.

A function $u : [0, T] \to \mathbb{R}^r$ represents a control strategy for system (1.1)-(1.2) and returns the value of the control vector at each point in the time horizon. Such a control strategy is called a control function and it is usually bounded. Hence, we normally assume that the range of the control function is contained within some proper subset $U = \{u = [u_1, \ldots, u_r]^T : \alpha_i \leq u_i \leq \beta_i, i = 1, \ldots, r\} \subset \mathbb{R}^r$, which is called the control restraint set. Here, α_i and β_i are given constants such that $\alpha_i < \beta_i$ for each $i = 1, \ldots, r$. A bounded measurable function $u : [0, T] \to U$ such that $u(t) \in U$ for all $t \in [0, T]$ is called an admissible control. Let $\mathcal{U}$ be the class of all such admissible controls.

The control function influences the state through the dynamic system (1.1). In other words, the control changes its value during the time interval $[0, T]$ which, in turn, affects the evolution of the state $x(t)$ according to the dynamic system (1.1) and (1.2). Let $x(\cdot|u)$ denote the solution of (1.1) and (1.2) corresponding to $u \in \mathcal{U}$.

Many practical problems include a variety of different constraints imposed on the state and control. A canonical form for system constraints can be mathematically expressed as:

$$G_i(u) = \Phi_i(x(T)) + \int_0^T L_i(t, x(t), u(t))dt \begin{cases} = 0, & i = 1, \ldots, q_e, \\ \geq 0, & i = q_e + 1, \ldots, q, \end{cases} \tag{1.3}$$

where q is the total number of canonical constraints and q_e is the number of canonical equality constraints. In an optimal control problem, we seek to optimize a cost functional of the form

$$G_0(u) = \Phi_0(x(T)) + \int_0^T L_0(t, x(t), u(t))dt. \tag{1.4}$$

Here, Φ_i and $L_i, i = 0, 1, \ldots, q$, are given continuously differentiable functions with respect to all their arguments. Thus, we state the general formulation of an optimal control problem as choosing a control $u \in \mathcal{U}$ so as to minimize the objective (1.4) subject to the dynamics (1.1) and (1.2) and subject to the constraints (1.3). Let this be denoted as Problem P_1. Analytical solutions of Problem P_1 are only possible for simple cases. These normally require the first order necessary conditions of optimality (the Euler-Lagrange equations in the case of unconstrained problems or the Pontryagin Minimum Principle in the case of control bounds) or solutions of the Hamilton-Jacobi-Bellman (HJB) equation derived via the dynamical programming principle.

1.3 Numerical solution techniques

In general, it is difficult to solve optimal control problems analytically. Thus, numerical methods are required. Numerical methods are classified into two broad categories: direct and indirect methods. A thorough review for these methods and their various approaches is given in [48]. Essentially, in an indirect method, the first order optimality conditions are applied to the original problem, resulting in a two point boundary value problem (TPBVP). This can then be solved numerically with either shooting methods or multiple shooting methods. On the other hand, in direct methods, the control and/or the state of the optimal control problem are approximated via a discretization process. This leads to a discretized version of the problem which can then be regarded as a mathematical programming problem and solved numerically using a variety of techniques. When only the control is approximated, the direct method is referred to as a control parameterization method. When both the state and the control are discretized, the approach is known as a state discretization method. As the control parameterization approach will be adopted in this thesis, we give a more detailed review below.

1.3.1 Control parameterization

Control parameterization is one of the common techniques to solve optimal control problems numerically [55]. Let us consider its application to Problem P_1. The basic concept of this technique centers around two steps; partition the time horizon of a problem into a number of fixed subintervals, i.e. partition the time horizon $[0, T]$ into a set of points $P = \{\{\tau_0, \tau_1, \ldots, \tau_N\}, \tau_0 = 0, \tau_N = T, \tau_{j-1} < \tau_j, j = 1, \ldots, N\}$, where N is the number of intervals in the partition chosen by the user. We then approximate each control function $u_i(t), i = 1, \ldots, r$, by a combination of basis functions $\psi_j, j = 1, \ldots, N$, as follows:

$$u_i(t) = \sum_{j=1}^{N} \sigma_{ij}\psi_j(t), \quad j = 1, \ldots, N, i = 1, \ldots, r, \tag{1.5}$$

where $\sigma_{ij}, i = 1, \ldots, r, j = 1, \ldots, N$, are decision variables which need to be optimally chosen in order to minimize the objective function. Most applications of control parameterization are implemented with piecewise constant basis functions. However, the basis functions can take other forms such quadratic or cubic or non polynomial [25]. In the case of piecewise constant basis functions, we choose $\psi_j(t) = \chi_{[\tau_{j-1}, \tau_j)}$, where

$$\chi_{[\tau_{j-1}, \tau_j)}(t) = \begin{cases} 1, & \text{if} \quad t \in [\tau_{j-1}, \tau_j), \\ 0, & \text{otherwise}, \end{cases} \tag{1.6}$$

is the indicator function with respect to the interval $[\tau_{j-1}, \tau_j)$. The approximate control

function can then be written as:

$$u_i(t) = \sum_{j=1}^{N} \sigma_{ij} \chi_{[\tau_{j-1},\tau_j)}(t), \tag{1.7}$$

where $\alpha_i \leq \sigma_{ij} \leq \beta_j, i = 1, \ldots, r, j = 1, \ldots, N$. Let $\sigma_i = [\sigma_{i1}, \sigma_{i2}, \ldots, \sigma_{iN}], i = 1, \ldots, r$, and $\sigma = [\sigma_1^T, \sigma_2^T, \ldots, \sigma_r^T]^T$. Furthermore, let $x(\cdot|\sigma)$ denote the solution of (1.1) and (1.2) when the control is defined by (1.7). Then, the approximate problem resulting from control parameterization can be written as follows. Minimize

$$G_0^N(\sigma) = \Phi_0(x(T|\sigma)) + \int_0^T \tilde{L}_0(t, x(t|\sigma), \sigma) dt \tag{1.8}$$

subject to dynamical system,

$$\dot{x}(t) = \tilde{f}(t, x(t), \sigma), \quad t \in [\tau_{i-1}, \tau_i), \quad i = 1, \ldots, N, \tag{1.9}$$

the initial condition (1.2) and the canonical constraints

$$G_i^N(\sigma) = \Phi_i(x(T|\sigma)) + \int_0^T \tilde{L}_i(t, x(t|\sigma), \sigma) dt \begin{cases} = 0, & i = 1, \ldots, q_e, \\ \geq 0, & i = q_e + 1, \ldots, q, \end{cases} \tag{1.10}$$

where $\tilde{f}(t, x(t), \sigma)$ and $\tilde{L}_i(t, x(t|\sigma), \sigma), i = 0, \ldots, q$, denote the functions f and $L_i, i = 0, \ldots, q$, respectively, with the argument $u(t)$ replaced by the form (1.7). The resulting approximate problem, referred to as Problem P_2, is essentially a mathematical programming problem which depends on a finite number of decision variables. Once the gradients of this problem have been calculated via the formulation of Hamiltonian functions and the solution of costate dynamics [55], it can be solved numerically by using a gradient based optimization method like sequential quadratic programming (SQP) (see [35], [14], [43] and [51]). The optimal control software MISER3.3 [25] implements this approach.

1.3.2 MISER

The FORTRAN based optimal control software MISER was originally developed by K.L. Teo and C.J. Goh in 1988 [21]. This version of MISER essentially solves the Problem P_2 described in the last section. A much more comprehensive and user friendly version, MISER3, was created by L.S. Jennings in 1991 [24]. In 2004, the latest version of MISER (MISER3.3) was developed. It incorporated significant improvements such as allowing state jumps in the dynamic system and multiple characteristic times in the objective and constraints [25]. Thus, MISER3.3 has become a powerful software which can be used to solve a wide range of practical optimal control problems. As mentioned above,

MISER's theoretical basis is the control parameterization technique. It basically deals with three standard forms of constraints: canonical constraints of the form given above, continuous inequality constraints on the states and linear constraints involving only the controls. Users only require a basic knowledge of multi-variable calculus and elementary FORTRAN programming skills to solve problems with features allowed by MISER3.3. More complex problems that do not fit the standard framework of MISER3.3 can often be transformed into an equivalent standard form suitable for the software.

1.3.3 Additional features allowed in MISER3.3

MISER3.3 generates a numerical solution to the general continuous optimal control and optimal parameter selection problem in the form stated below. Here $(u, z) \in \mathcal{U} \times \mathcal{Z}$, where $u(t) \in \mathcal{U}$ is the control function as defined previously, and $z \in \mathcal{Z}$ is a vector of system parameters, where $\mathcal{Z}$=$\{z = [z_1, \ldots, z_m]^T : a_i \leq z_i \leq b_i, i = 1, \ldots, m\}$ is a set of feasible system parameters. The problem is to choose $(u, z) \in \mathcal{U} \times \mathcal{Z}$ to minimize

$$G_0(u, z) = \sum_{j=1}^{M} \Phi_{0,j}(x(\gamma_j), z) + \int_0^T L_0(t, x(t), u(t), z)dt \tag{1.11}$$

subject to the dynamic system,

$$\dot{x}(t) = f(t, x(t), u(t), z), \quad t \in [0, T], \tag{1.12}$$

the initial conditions

$$x(0) = x^0(z), \tag{1.13}$$

the canonical constraints

$$G_i(u, z) = \sum_{j=1}^{M} \Phi_{i,j}(x(\gamma_j), z) + \int_0^{\gamma_j} L_i(t, x(t), u(t), z)dt \begin{cases} = 0, & i = 1, \ldots, q_e, \\ \geq 0, & i = q_e + 1, \ldots, q, \end{cases} \tag{1.14}$$

and the continuous inequality constraints

$$h_i(x(t), z) \geq 0, \quad t \in [0, T], \quad i = 1, \ldots, n_c, \tag{1.15}$$

where

- f, L_i and $\Phi_{i,j}$ are given functions, assumed to be continuously differentiable with respect to x, u and z, and piecewise continuous with respect to time t;
- $\gamma_j, j = 1, \ldots, M$, are known as the characteristic times of the canonical constraints.

This problem is denoted as Problem P_3. In addition to the formulation above, MISER3.3 allows for a range of other features such as piecewise linear continuous control functions, jump conditions in the state dynamics and various types of regularization terms in the objective. We have not detailed these here as they are not used in the computational work for this thesis. However, the interested reader can find details in [25].

The continuous inequality constraints (1.15) are effectively infinite dimensional constraints for the underlying mathematical programming problem that results from the control parameterization method. An early approach [54] transformed these constraints into a canonical form (1.14), but the resulting constraints are not differentiable and can thus cause numerical difficulties for the nonlinear programming solver built into MISER. A more comprehensive transcription technique which involves two smoothing parameters was proposed in [56]. This has been coded into the MISER package and the user merely needs to specify the right hand side of (1.15) and set a switch to invoke this technique. A more thorough theoretical analysis of the technique which demonstrates that controls may also be included in the right hand side of (1.15) was given in [32].

The use of multiple characteristic time points in the objective and constraints was first proposed in [41] where gradient formula for such functionals were derived. Once again, these have been incorporated into the MISER software so that the user merely needs to specify the existence of the multiple characteristic time points.

To use MISER3.3, the user needs to edit a given file of FORTRAN subroutines which is then compiled into an executable program with the rest of the MISER code. Essentially, the user has to code up all functions in the dynamics, objective and constraints as well as their first order derivatives with respect to the states, controls and system parameters. MISER then uses these to construct and solve a parameterized version of the problem. This involves setting up the co-state differential equations, solving the state and co-state dynamics numerically, evaluation of the objective and constraints, formulation and evaluation of gradients of the objective and constraints with respect to all decision variables and finally the optimization of the underlying mathematical programming problem via sequential quadratic programming (SQP) [50]. Note also that other information about a problem, such as the number of states, controls, system parameters and constraints, the constraint types, control and system parameter bounds, partitioning of the time horizon for control parameterization, options for the numerical solution of the dynamics, and options for the optimization routine are specified by the user in a data file that can be easily constructed when the executable code is first invoked.

It should be noted that the numerical solution of general combined optimal control and optimal parameter selection problems is a complex task even with the availability of packages like MISER3.3. Convergence to an optimal solution may be slow and some judgment on the part of the user is required to set appropriate parameters for the optimization

processes and to determine when the number of iterations is sufficient. Furthermore, since the underlying mathematical programming problem is non-convex, convergence may only lead to locally optimal solutions and it may be necessary to start the process with several initial guesses to find a good solution.

In practice, the accuracy of the optimal control obtained by the standard control parameterization method with piecewise constant controls is often not high, as it is impossible to know the precise switching times a priori. To obtain higher accuracy, the switching times of the controls should also be regarded as decision variables, but MISER3.3 does not allow for this possibility. However, as detailed in the next section, this difficulty can be overcome via a time scaling transformation which was originally proposed in [29]. As we will see later in the thesis, the same technique can also be employed to allow for variable characteristic times in both the objective and the constraint functionals.

1.3.4 Time scaling transformation

For ease of notation, we illustrate the application of the technique to Problem P_1 only. Suppose that we implement control parameterization for Problem P_1 using the partition P defined in Section 1.3.1 and the piecewise constant control given by (1.7). We now want the points in the partition $\tau_i, i = 1, \ldots, N$ to be variables also. Thus, we invoke a well known transformation [30] to map these variable time points to fixed points on a new time horizon $[0, N]$. The resulting equivalent problem avoids several numerical difficulties associated with variable switching times [30] and can be solved directly with MISER3.3. This is achieved by defining a new time variable $s \in [0, N]$, a set of equivalent variables

$$\theta_i = \tau_i - \tau_{i-1}, \quad i = 1, \ldots, N, \tag{1.16}$$

and setting

$$\frac{dt(s)}{ds} = v(s), \tag{1.17}$$

where $v : [0, N] \to \mathbb{R}$ is a piecewise constant function defined by

$$v(s) = \sum_{i=1}^{N} \theta_i \chi_{[i-1,i)}(s), \tag{1.18}$$

which satisfies the bounds

$$0 \leq v(s) \leq T, \quad s \in [0, N]. \tag{1.19}$$

As before, the indicator function is defined as

$$\chi_{[i-1,i)}(s) = \begin{cases} 1, & \text{if} \quad s \in [i-1, i), \\ 0, & \text{otherwise.} \end{cases} \tag{1.20}$$

Furthermore, we require

$$t(0) = \tau_0 = 0, \tag{1.21}$$

and

$$t(N) = T. \tag{1.22}$$

Note that $\theta_i, i = 1, \ldots, N$, are now decision variables in the transformed problem and the values of $\tau_i, i = 1, \ldots, N$, can be easily calculated from $\theta_i, i = 1, \ldots, N$. Furthermore, we require

$$0 \leqslant \theta_i \leqslant T, \quad i = 1, \ldots, N. \tag{1.23}$$

Let $\tilde{x}(s) = x(t(s))$ and $\tilde{u}(s) = u(t(s))$.

Since (1.17) can be re-arranged as $dt = v(s)ds$, the transformed problem is to choose a control of the form (1.7) (i.e. choosing both σ_{ij} and $\theta_i, i = 1, \ldots, N$) to minimize the objective

$$\tilde{G}_0 = \Phi_0(\tilde{x}(N)) + \int_0^N v(s) L_0(t(s), \tilde{x}(s), \tilde{u}(s)) ds \tag{1.24}$$

subject to the dynamic system

$$\dot{\tilde{x}}(s) = v(s) f(t(s), \tilde{x}(t), \tilde{u}(s)), \tag{1.25}$$

differential equation (1.17), the initial conditions (1.2) and (1.21), the constraints

$$\tilde{G}_i = \Phi_i(\tilde{x}(N)) + \int_0^N v(s) L_i(t(s), \tilde{x}(s), \tilde{u}(s)) ds \begin{cases} = 0, & i = 1, \ldots, q_e, \\ \geq 0, & i = q_e + 1, \ldots, q, \end{cases} \tag{1.26}$$

the constraint (1.22) and the bounds on v (1.19) and θ (1.23). Note that the transformed problem fits directly into the general MISER3.3 framework. Compared to Problem P_2, the revised problem, denoted as Problem P_4, has one additional state, one additional control function and one additional canonical constraint.

Finally, note that the same time scaling transformation can also be employed for more general classes of optimal control problems such as Problem P_3 described in Section 1.3.3.

CHAPTER 2

Literature Review

2.1 Mathematical modelling of the blood glucose regulatory system

A range of mathematical models have been proposed in the literature to capture, and, in many cases, control blood glucose dynamics in the human body. Most of these are dynamic in nature, either in the form of differential or difference equations. They often include other compounds associated with glucose, such as insulin, glucagon and glycogen. Some models are designed exclusively to determine treatment regimes for Type 1 diabetics while others are intended for both healthy individuals as well as those with a diabetic impairment. Models also differ in terms of the processes that they capture. For example, some models simply assume the appearance of glucose in the blood while others actually capture the digestive process directly. Models vary greatly in terms of their complexity, ranging from simple linear models involving just glucose and insulin [1] to complex nonlinear models which try to capture the chemical changes of the beta cells in the pancreas [20]. While simple linear models lend themselves to analytic analysis and the application of standard control algorithms from the engineering disciplines, they do not capture the rich dynamic behavior of the real process. There is an ever expanding range of medical treatment options for diabetes beyond the traditional use of insulin. In order to capture the various effects of these treatments, mathematical models must include those dynamics which are directly affected by the treatments. In this chapter, we review a range of existing models and outline their main features.

2.1.1 Bergman minimal model

The Bergman minimal model [10] was proposed around 1980 to allow researchers to measure the quantitative contributions of pancreatic responsiveness (i.e. the increased production of insulin by the pancreas) and insulin sensitivity (i.e. the increased uptake of glucose by cells in response to insulin) to a subject's overall glucose tolerance (i.e. the

body's ability to revert from high blood glucose levels back to base levels). As both of these effects lead to a lowering of blood glucose levels, it is generally difficult to measure their relative contribution. The proposed model is 'minimal' in the sense that it is the simplest physiologically based representation of the blood glucose regulatory system which can account for the following factors:

(a) observed glucose kinetics when the plasma insulin values are supplied; and

(b) observed insulin kinetics when the plasma glucose values are supplied.

The minimal model was used in [10] to estimate the characteristic parameters of pancreatic responsiveness and insulin sensitivity of several subjects who underwent an intravenous glucose tolerance test (IVGTT) and whose plasma glucose and insulin levels were measured in response to the IVGTT. Up until the results in [10], quantitative analysis of pancreatic responsiveness and insulin sensitivity was only possible by artificially maintaining constant blood glucose levels (by infusion of glucose during an experiment, known as glucose clamp) which entailed some risk to the subject. Despite the limited intended application of the Bergman minimal model as an analysis tool for IVGTT data, its inherent simplicity (it involves only 3 coupled ordinary differential equations) has led to many researchers adopting and modifying the model in subsequent publications. In [9], more than 500 such studies have been identified in the literature. It is also worth noting that the role of the liver in the blood glucose regulatory system is acknowledged in [10], although it is not included in the minimal model. Although no direct treatment methods are proposed in [10] for glucose intolerant (i.e.diabetic) subjects, it is noted that once a subject's pancreatic responsiveness and insulin sensitivity have been identified, specific treatments can be designed with more confidence. The dynamic system takes the following form [12]:

$$\frac{dG}{dt} = -p_1[G(t) - G_b] - X(t)G(t) + D(t), \tag{2.1}$$

$$\frac{dX}{dt} = -p_2 X(t) + p_3[I(t) - I_b], \tag{2.2}$$

$$\frac{dI}{dt} = \begin{cases} \gamma[G(t) - h]t - h[I - I_b], & \text{if} \quad G(t) - h > 0, \\ -n[I - I_b] + u(t), & \text{if} \quad G(t) - h \leq 0, \end{cases} \tag{2.3}$$

where

$G(t)[mg/dl]$ = the blood glucose concentration at time t [min];

$I(t)[\mu U/ml]$ = blood insulin concentration at time t (min);

$X(t)[\text{min}^{-1}]$ = a function representing insulin excitable tissue glucose uptake activity, proportional to insulin concentration in a remote compartment;

$G_b[mg/dl]$ = the subject's basal glucose level;

$I_b[\mu U/ml]$ = the subject's basal insulin level;

$D[mg/dl]$ = exogenous infusion of glucose;

$u(t)[\mu U(ml])$ = exogenous infusion of insulin; the basal glucose and insulin levels refer to the intravenous glucose tolerance test (IVGTT) record;

$n[min^{-1}]$ = the time constant for insulin decay;

$p_1[min^{-1}]$ = the insulin independent rate constant of glucose uptake in muscles and liver;

$p_2[min^{-1}]$ = the rate of decrease in the tissue glucose uptake ability;

$p_3[(\mu U(ml)min^{-2})]$ = the insulin dependent increase in glucose uptake ability in tissue per unit of insulin concentration above the basal level;

$h[mg/dl]$= the pancreatic "target glycaemia";

$\gamma[(\mu U/ml)/(mg/dl)^{-1}min^{-1}]$= the rate of pancreatic release of insulin after the bolus of glucose concentration above the target "glycaemia".

Here, U is the international unit especially for insulin, such that $1mU = 6.945 \times 10^{-12}M$.

Equation (2.1) assumes the appearance of glucose via the digestion of a meal and two means by which glucose disappears, one related to insulin and the other unrelated. Equation (2.2) assumes a natural decay of remote insulin and appearance/disappearance of glucose depending on its current level in relation to a basal level. Equation (2.3) describes the dynamics of pancreatic insulin release in response to glucose stimulus for two cases, a healthy person and a diabetic. The term $\gamma[G(t) - h]t$ presents endogenous insulin secretion for a healthy person in the first case (when $G(t) - h > 0$) and it does not appear in the second case which describes the insulin release rate for a diabetic. In contrast, the term $u(t)$ which represents an exogenous infusion of insulin is added in this second case.

2.1.2 Models by Cobelli and coworkers

A more comprehensive model of the blood glucose regulatory system which considers glucagon dynamics alongside insulin dynamics and their interrelation was proposed in [13].

This model involves three subsystems. The glucose subsystem is described by a one-compartment model of distribution and metabolism that involves net hepatic glucose balance (i.e. the difference between liver glucose production and uptake), renal excretion of glucose, insulin-dependent glucose utilization (by muscle) and insulin-independent glucose utilization (by the central nervous system). The insulin subsystem is described by a five-compartment model that involves pancreatic insulin storage, liver and portal plasma insulin, plasma insulin and insulin in the interstitial fluid. The glucagon subsystem is described by a one-compartment model that involves plasma glucagon and glucagon in the interstitial fluid.

The authors in [13] acknowledge the difficulty of validating complex models against experimental data. However, they point out that many aspects of their model are based on results from both whole body and individual organ experiments. Reference [13] also includes a range of simulations of their model for a variety of different scenarios and demonstrates reasonable results in each case. While acknowledging some shortcomings of their model, the authors of [13] make an important point which is true for any comprehensive mathematical model in the biological sciences: *'The usefulness of the model as a sort of efficient and integrated library of physiological and clinical knowledge in a research group working both experimentally and theoretically on carbohydrate metabolism can not be overemphasized'*. Despite its complexity (or perhaps because of it), the model in [13] has not been as widely cited as the Bergman minimal model. Its distribution of insulin into five compartments is unique amongst all the models we have studied and this feature was never carried forward into future models that evolved from the group of researchers around Claudio Cobelli. A recent example is proposed in [37] where several independent sub-models are combined. One of these sub-models describes the glucose ingestion and absorption processes in the digestive system, a difficult task in its own right. The model in [37] was fitted to the results of a comprehensive experiment involving over 200 healthy and 14 type 2 diabetic subjects who consumed a meal with 3 versions of traceable glucose. The aim of the resulting model is to serve as a simulation tool for testing various types of diabetic treatment regimes. For this purpose, a Matlab version of the models, known as GIM [15], has been created for general use by researchers.

2.2 Early work on diabetes control

There were several publications by M.E. Fisher around 1990 with the aim to derive optimal strategies for the control of diabetes. Both analytical and numerical solution methods were employed, including the first ever application of computational optimal control methods in this area. In [18], the simple linear dynamic model of [1] was employed to describe the glucose dynamics while [17] makes use of the nonlinear Bergman minimal model [10]. The

scenarios tested essentially assumed a type 1 diabetic subject and the requirements were to reduce an initially high blood glucose level in one case or to deal with a glucose spike due to a meal ingested in another case. The only means of controlling blood glucose was assumed to be the external administration of insulin. Some interesting results were obtained, such as the superiority of single large dose of insulin over a continuous injection but the underlying models were too simple to justify any conclusions in a realistic environment.

2.3 Blood glucose control for diabetics

Many of the proposed mathematical models for the blood glucose regulatory system were constructed with the ultimate purpose of determining various ways of controlling glucose levels for diabetic patients (mainly via appropriate injections of insulin). An excellent review of a range of control algorithms can be found in [12], where the authors also discuss in detail the glucose measuring devices and insulin injection equipment used in clinical settings. We give a brief review of several control methods below.

A range of model free control algorithms has been described in the literature, mainly in the context of type 1 diabetic treatment. Model free means that the algorithms are not based on any mathematical model of the glucose regulatory system. Instead, they generally rely on frequent blood glucose measurements, including the response of blood glucose levels to known quantities of insulin infusions. Simple versions rely on look up tables or functional curves based on previous experience while more advanced ones employ methods popular in engineering such as proportional-integral-derivative (PID) control or neural network approaches (where a neural network is first trained on the insulin-glucose response data) [12]. While these model free algorithms are usually easy to implement in practice and can, with some experience, lead to good blood glucose control, they are effectively a black box approach and offer no insights into how the real underlying system functions [12].

In contrast, model based control methods assume a mathematical model of the glucose regulatory system and can thus deal with more complicated scenarios such as model disturbances or other major perturbations of the system. Drawbacks of the model based approach are that the model may lack validity or accuracy and that models often contain multiple uncertain parameters that may be difficult to measure in practice. Several recent approaches are outlined below.

In [46], discrete time model based algorithms for type 1 diabetic patients fitted with closed loop insulin infusion pumps are proposed. A linear state space model is assumed and used to estimate future output values based on a series of past inputs. This information is then used to generate a linear model predictive controller (MPC). This approach is then enhanced with the use of a Kalman filter for state estimation and the non lin-

ear quadratic dynamic matrix control (NLQDMC) technique (which compensates for the known non linearities of the process). The digital nature of this algorithm lends itself to possible implementation via micro chips. A similar MPC based approach is used in [36], where the authors augment the state space model with an additional differential equation which models the relationship between the blood glucose levels in the subcutaneous layer (where measurements are taken from in practice) and in the blood plasma.

A non linear model predictive controller was proposed in [23] with the aim of maintaining normal blood glucose levels in type 1 diabetic patients during fasting conditions. It is based on the authors' own blood glucose regulatory model which also includes a two compartment submodel to represent the absorption of subcutaneously administered insulin. Other features of the model are of a similar level of complexity as the Bergman minimal model [10]. An interesting feature of the controller proposed in [23] is the provision of target trajectories towards the desired normal blood glucose level of 6 (mmol/L). A linear decrease is prescribed for high blood glucose concentrations while a logistic increase is prescribed when starting with low concentrations. The actual implementation of the controller in [23] is over discrete time steps. An important point made by the authors of [23] is that the parameters of their underlying model need to be chosen and fitted separately for every individual patient. Indeed, they may even need to be recalculated for the same patient over longer time periods. This observation can be readily applied to all models of the blood glucose regulatory system.

In [39], the authors augment the Bergman minimal model with an additional equation to describe endogenous insulin production so that they can also capture the behavior of type 2 diabetic patients. They then derive a proportional derivative (PD) and a model predictive controller (MPC) on the basis of the augmented model and propose a switching control strategy which attempts to balance optimal performance with reduced computational complexity and the need to avoid hypoglycemia. Results are shown to be a significant improvement over those obtained from more traditional PD controllers. This is one of the few control papers concerned with type 2 diabetic patients.

Both [47] and [28] propose a similar control approach based on the H_∞ criterion in linear control system design. In [28], the linear system is based on a series of set points derived from the non linear model in [31] (which we will review in more detail in the next section). In [47], the authors linearized the comprehensive nonlinear model of [53]. Both algorithms were extensively tested on perturbed versions of their underlying nonlinear models and found to perform well. An interesting feature of [47] was the inclusion of lactate (which appears in the blood stream in response to moderate exercise) and adrenaline (which appears in the blood stream in response to nocturnal hypoglycemic episodes) in their linearized model.

A rather different control approach was proposed in [5]. The problem of determining

an optimal closed loop control for an underlying non linear model of blood glucose can, in principle, be addressed by dynamic programming. However, the computational cost of this direct approach is prohibitive for most practical problems. Instead, the authors of [5] adopt an approximate dynamic programming (ADP) formulation and the solution is obtained via a neural network approach. Since the neural network can be trained off line, the overall method is suitable for real time application. Results in [5] show that the strategy performs significantly better than other control strategies based on linearized approximations of the underlying model. In particular, it is better at avoiding the crucial problem of hypoglycemia. However, the approach was based on a relatively simple version of the Bergman minimal model and it was not tested in clinical trails.

Despite a large range of control algorithms being available, the utopian notion of an artificial pancreas which requires no intervention is still some time away. In addition to a control algorithm, such a device also requires continuous blood glucose (BG) sensors and an insulin pump to deliver the insulin to the subject (patient). While subcutaneous insulin pumps are nowadays widely used in type 1 diabetics and have proven reliability, the task of measuring blood glucose levels is more difficult.

Various blood glucose monitoring techniques have been developed to date and they can be classified into three categories. Firstly, invasive techniques depend on taking regular blood glucose (BG) samples directly from veins and sending these samples to a glucose sensor. The time delay due the time taken by the sensor has been reduced over the years from about 10 minutes to about 50 seconds for modern devices. Because the BG measurement is done in the actual fluid of interest invasive methods have high accuracy. However, there are some disadvantages such as the need for medical supervision, significant loss of blood with frequent sampling, and the risk of infections and thrombosis.

Secondly, there are the minimally invasive techniques. These are safer than invasive methods because the BG measurement is implemented outside the vascular tree, so it avoids the risks associated with accessing veins. The basic idea is to measure BG indirectly via accessing veins the subcutaneous (SC) layer. Based on this measurement, one can deduce BG levels based on the relationship between the subcutaneous glucose and the plasma glucose levels. Many studies have investigated this relationship [36]. The measurement can be taken via a glucose sensor implanted in the SC tissue or via fluid extracted from the SC space. For the case of sensors implanted into the SC tissue, the measurement is done in situ by using methods such as amperometry (an example of such a sensor is the MiniMed Continuous Glucose Monitoring System (CGMS)) or fluorescence detection. The implantable sensors have some advantages due to their small size and portability and they do not require extraction of SC fluid for operation. In contrast, some problems can occur with implanted sensors such as inflammation and membrane biofouling. Biofouling is a common problem which involves the gradual accumulation of proteins and biological

organisms on the sensor surface which reduces the accuracy of the sensor signal. Also, note that the need to compute the BG level from the SC level via a mathematical model requires some effort and may not always give accurate results.

The last category of BG measurement techniques are the non-invasive ones. Clearly, any patient would prefer to measure blood glucose by a painless method which does not require puncturing the skin or other forms of discomfort. An example of a non-invasive technique is optical spectroscopy. This is based on the optical properties of glucose when exposed to radiation. In other words, it is possible to determine blood glucose levels by exposing tissue to radiation. Many studies based on the optical spectroscopy method have appeared in the literature. A comprehensive review of these methods and their various applications is given in [12]. Another non-invasive technique is dielectric spectroscopy. In this technique, a small alternating current (AC), is applied and the impedance of the tissue to the current flow is recorded as a function of frequency [52]. Skin impedance is very sensitive to changes in membrane potential which is, in turn, influenced by the interaction of glucose with red blood cells. Thus, blood glucose levels can be deduced on the basis of the impedance data. Noninvasive techniques are still being improved and are the subject of current research with few clinical applications.

2.4 Model by Liu and Tang

A large proportion of the computational work in this thesis is based on the blood glucose regulatory model proposed by Liu and Tang in [31]. This nonlinear model is considered to be of an intermediate level of complexity. It supersedes the Bergman minimal model by also taking into account the dynamics of glucose and glycogen in the liver as well as the dynamics of insulin and glucagon receptors at the molecular level, but it has less state variables than the complex model proposed by Sorenson [53].

The dynamic model in Liu and Tang [31] consists of eight state variables. These state variables are defined as follows:

x_1 = concentration of plasma glucagon (in moles per liter);

x_2 = concentration of plasma insulin (in moles per liter);

x_3 = intracellular concentration of glucagon (in moles per liter);

x_4 = intracellular concentration of insulin (in moles per liter);

x_5 = concentration of glucagon receptor (in moles per liter);

x_6 = concentration of insulin-bound receptor (in moles per liter);

x_7 = blood concentration of glycogen (in milligrams per liter);

x_8 = blood concentration of glucose (in milligrams per liter).

The model can be naturally divided into three subsystems, each of which is described below. See Figure 2.1 for a graphical representation.

The insulin and glucagon transition subsystem governs x_1 and x_2. The model assumes that plasma insulin does not act directly on the glucose metabolism, but instead through remote cellular insulin. The model also assumes that intracellular insulin does not move back to plasma. Under these assumptions, the dynamics for x_1 are given by

$$\frac{dx_1}{dt} = -(k^p_{1,1} + k^p_{1,2})x_1 + w_1, \tag{2.4}$$

where $k^p_{1,1}$ is a transition rate, $k^p_{1,2}$ is a degradation rate, and w_1 is the glucagon release rate (GRR) defined by

$$w_1 = \frac{G_m}{1 + b_1 \exp a_1(x_8 - C_5)}. \tag{2.5}$$

Furthermore, the dynamics for x_2 are given by

$$\frac{dx_2}{dt} = -(k^p_{2,1} + k^p_{2,2})x_2 + w_2, \tag{2.6}$$

where $k^p_{2,1}$ is a transition rate, $k^p_{2,2}$ is a degradation rate, and w_2 is the insulin release rate (IRR) defined by

$$w_2 = \frac{R_m}{1 + b_2 \exp a_2(C_1 - x_8)}. \tag{2.7}$$

The fractions w_1 and w_2 in equations (2.4)-(2.7) model the natural feedback control mechanisms in the body. Note that G_m is the maximum glucagon infusion rate, R_m is the maximum insulin infusion rate, and a_1, a_2, b_1, b_2, C_1 and C_5 are positive constants.

The insulin and glucagon receptor binding subsystem governs x_3, x_4, x_5 and x_6. The model assumes that receptor recycling is a closed subsystem; the synthesis rate of receptors is equal to their degradation rate. The dynamics for this subsystem are given by

$$\frac{dx_3}{dt} = -k^s_{1,1}x_3(R^0_1 - x_5) - k^s_{1,2}x_3 + \frac{k^p_{1,1}V_p x_1}{V}, \tag{2.8}$$

$$\frac{dx_4}{dt} = -k^s_{2,1}x_4(R^0_2 - x_6) - k^s_{2,2}x_4 + \frac{k^p_{2,1}V_p x_2}{V}, \tag{2.9}$$

$$\frac{dx_5}{dt} = -k^s_{1,1}x_3(R^0_1 - x_5) - k^r_1 x_5, \tag{2.10}$$

$$\frac{dx_6}{dt} = -k^s_{2,1}x_4(R^0_2 - x_6) - k^r_2 x_6, \tag{2.11}$$

where $k^s_{1,1}$ and $k^s_{2,1}$ are the hormone-receptor association rates, $k^s_{1,2}$ and $k^s_{2,2}$ are the degradation rates, R^0_1 and R^0_2 are the total concentrations of receptors, k^r_1 and k^r_2 are the

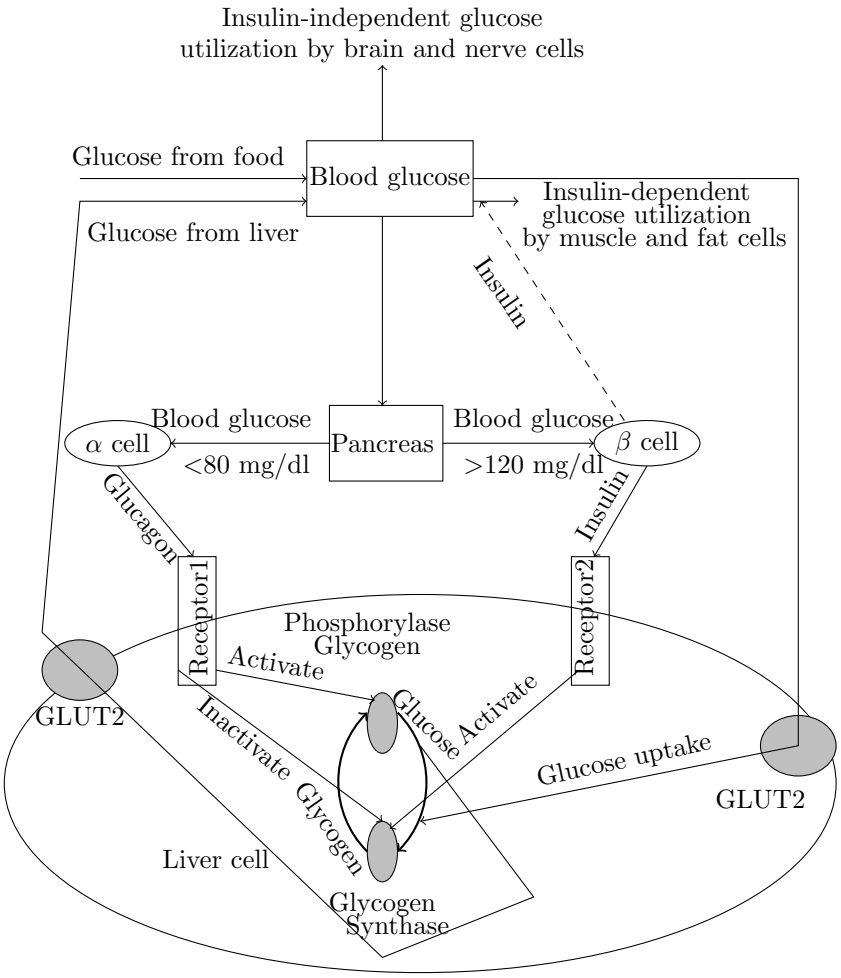

Figure 2.1: A simplified model of the regulatory system for blood glucose (adapted from reference [31]). Glucose is input from food and the liver, and used by brain and nerve cells (insulin-independent) and by tissue cells such as muscle, kidney, and fat cells (insulin-dependent, indicated by the dashed arrow). Glucose is transported to and from liver cells by the concentration-driven GLUT2, which is insulin-independent. In response to low blood glucose levels (< 80 mg/dl), the α cells of the pancreas produce the hormone glucagon. The glucagon initiates a series of activations of kinases (the black arrows indicate such activations). This ultimately leads to the activation of the enzyme glycogen phosphorylase, to catalyze the breakdown of glycogen into glucose. In addition, the series of activations of kinases also result in the inhibition of glycogen synathase, which stops the conversion of glucose to glycogen. In response to high blood glucose levels (> 120 mg/dl), the β cells of the pancreas secrete insulin. Insulin triggers a series of reactions to activate glycogen synthase, which catalyzes the conversion of glucose into glycogen.

inactivation rates, V_p is the plasma insulin volume, and V is the cellular insulin volume.

The glucose production and utilization subsystem governs x_7 and x_8, and thus models the production of glucose. Plasma glucose has two sources: hepatic glucose produced by converting glycogen into glucose in the liver represented by f_5 defined in equation (2.12)

and exogenous glucose taken from food represented by G in equation (2.15). Glucose utilization can be classified into two classes: insulin-independent (by the brain and nerve cells) (represented by f_1 defined in equation (2.16)) and insulin-dependent (by the muscle and fat cells) (represented by the product of f_2 and f_3, themselves defined in equations (2.17) and (2.18)). The dynamics for x_7 are given by

$$\frac{dx_7}{dt} = f_4 - f_5, \tag{2.12}$$

where

$$f_4 = \frac{k_1 x_6}{1 + k_2 x_5} \cdot \frac{V_{\max}^{gs} x_8}{k_m^{gs} + x_8} \tag{2.13}$$

represents the synthasis of glycogen from glucose and

$$f_5 = k_3 x_5 \frac{V_{\max}^{gp} x_7}{k_m^{gp} + x_7}. \tag{2.14}$$

Here, k_1, k_2 and k_3 are the feedback control gains, $V_{\max}^{gs}$ is the maximum velocity of glycogen phosphorylase, $V_{\max}^{gp}$ is the maximum velocity of glycogen synthase, and k_m^{gs} and k_m^{gp} are the Michaelis-Menton constants.

The dynamics for x_8 are given by

$$\frac{dx_8}{dt} = -f_4 + f_5 - f_1 - f_2 f_3 + G, \tag{2.15}$$

where

$$f_1 = U_b \left(1 - \exp\left(-\frac{x_8}{C_2}\right)\right), \tag{2.16}$$

$$f_2 = \frac{x_8}{C_3}, \tag{2.17}$$

$$f_3 = U_0 + \frac{(U_m - U_0) x_4^{\beta}}{C_4^{\beta} + x_4^{\beta}}. \tag{2.18}$$

Note that U_0, U_b, U_m, C_2, C_3, C_4 and β are positive constants, and G is the exogenous glucose intake derived from digesting food. Note also that t is the time in minutes.

The initial conditions prescribed for the model in Liu and Tang [31] are

$$x_1(0) = 1.4 \times 10^{-11}, \tag{2.19}$$
$$x_2(0) = 2 \times 6.945 \times 10^{-12}, \tag{2.20}$$
$$x_3(0) = 0, \tag{2.21}$$
$$x_4(0) = 0.01 \times 6.945 \times 10^{-12}, \tag{2.22}$$
$$x_5(0) = 0, \tag{2.23}$$
$$x_6(0) = 0, \tag{2.24}$$
$$x_7(0) = 200, \tag{2.25}$$
$$x_8(0) = 918. \tag{2.26}$$

The complete model defined by equations (2.4)-(2.26) includes 36 model constants.

The model incorporates a number of features that distinguishes it from earlier ones. In particular, Liu and Tang assume inherent feedback rates for glucagon and insulin (w_1 and w_2, respectively) which model the body's own regulating controls. Based on their model, Liu and Tang develop a new formula to quantify the insulin sensitivity of a subject and they also demonstrate that their feedback model is input-output stable. This stability gives theoretical support to the knowledge that blood glucose in a healthy individual fluctuates in a narrow range and further supports the applicability of the model. Finally, Liu and Tang proposed an optimal control problem based on their model with a quadratic performance index, but they considered this problem too difficult to solve because of the complexities and nonlinearities in the model.

2.5 Contributions of the thesis

As we have clearly shown above, there are already many publications devoted to the problem of controlling blood glucose in diabetic patients. However, very few of the algorithms preserved are based directly on underlying nonlinear models and thus they cannot take full advantage of the assumed nonlinearities. The only contribution of those reviewed above which uses computational optimal control methods on the basis of a nonlinear model is [17]. Since its publication, significant advances have been made in the area of computational optimal control. In particular, we are now able to deal with problems with variable decision points in the time horizon and these time points may also appear in the objective function and in the dynamics.

Thus, the first aim of this thesis is to demonstrate that computational optimal control methods can be readily used to determine open loop optimal controls for models of the blood glucose regulatory system. While open loop controls do not take into account

modelling errors and uncertainties in systems, they still provide a useful benchmark for the performance of other more direct control strategies. Using this approach, we can also test extreme scenarios on models and thus identify their weaknesses.

In Chapter 3, we first formulate and solve an optimal parameter selection problem in order to obtain more suitable values for many of the model parameters in the Liu and Tang model. It is generally acknowledged in biological modelling that model constants are difficult to determine exactly on the basis of experimental results. In the case of blood glucose models, it has also been noted that model constants can vary significantly between different subjects and over time for the same subject. We also show that, unlike the perception raised in [31], optimal controls for insulin and glucagon are readily obtained by standard computational methods.

In Chapter 4, our aim is to expand the Liu and Tang model in two ways in order to develop effective optimal control strategies for the treatment of diabetic subjects. One of the treatment options is increased levels of exercise. The range of dynamic models incorporating exercise is limited and we review several examples before adopting one approach and combining it with the Liu and Tang model. The second form of treatment is assumed to be via bolus insulin injections. As the Liu and Tang model does not incorporate insulin injection dynamics, we review a range of potential models and adopt a suitable candidate. We then formulate a combined optimal control and optimal parameter problem with the aim of determining combined optimal exercise and insulin treatment strategies for various patient scenarios. Using a time scaling transformation, we show that the resulting problem is readily solvable via the optimal control software MISER3.3 .

While our studies are primarily based on the model by Liu and Tang, our overall methodology and the computational tool we used can be applied to any blood glucose model. We identify a number of future research directions in Chapter 5 in terms of future possible changes to the Liu and Tang model in order to incorporate a broader range of diabetic treatment regimes.

CHAPTER 3

Modelling and Optimal Control of Blood Glucose Levels in the Human Body

3.1 Introduction

Regulating the blood glucose level is a challenging control problem for the human body. Abnormal blood glucose levels can cause serious health problems over the short and long term. Although several mathematical models have been proposed to describe the dynamics of glucose-insulin interaction, none has been universally adopted by the research community. In this chapter, we consider a dynamic model of the blood glucose regulatory system originally proposed by Liu and Tang in 2008. This model consists of eight state variables naturally divided into three subsystems: the glucagon and insulin transition subsystem, the receptor binding subsystem and the glucose subsystem. The model contains 36 model parameters, many of which are unknown and difficult to determine accurately. We formulate an optimal parameter selection problem in which optimal values for the model parameters must be selected so that the resulting model best fits given experimental data. We demonstrate that this optimal parameter selection problem can be solved readily using the optimal control software MISER3.3. Using this approach, significant improvements can be made in matching the model to the experimental data. We also investigate the sensitivity of the resulting optimized model with respect to the insulin release rate. Finally, we use MISER3.3 to determine optimal open loop controls for the optimized model.

To date, several mathematical models for the blood glucose regulatory system have been proposed. These models aim to describe the glucose-insulin interaction within the human body. The Bergman minimal model (1980) is considered to be the fundamental model in this area [12]. Several control models, such as proportional-integral-derivative (PID) control [38], robust servo control [28], and model predictive control (MPC) [23], have been developed based on the Bergman minimal model. In most of the existing models, the glucose regulatory system is greatly simplified and only glucose and insulin

are considered.

Liu and Tang [31] have developed a new feedback control model at the molecular level, which considers the role of the liver, the glucagon and insulin signaling pathways and the conversion between glucose and glycogen. However, one of the difficulties in working with this model is that it contains many model parameters whose values are not well-defined. Thus, in this chapter, we formulate an optimal parameter selection problem that can be solved using the software package MISER3.3 [25]. As we will see, this approach results in significant improvements in matching the model to experimental data.

This chapter is organized as follows. We first review the dynamic model of blood glucose levels proposed in [31] in Section 3.2. Then, in Section 3.3, we formulate an optimal parameter selection problem to determine optimal values for the uncertain model parameters in the dynamic model. The objective here is to match the model to given experimental data as closely as possible. For this purpose, we consider three possible objective functions and solve the resulting problems using MISER3.3. In Section 4.4, we perform a sensitivity test, as proposed in Liu and Tang [31], on the resulting optimized model to test its sensitivity with respect to the insulin release rate. In Section 3.5, based on the optimized model, we formulate an optimal control problem in which the aim is to optimize the release rate for both insulin and glucose. This optimal control problem can also be solved using MISER3.3. Finally, we conclude the chapter with a discussion of the numerical results.

3.2 Mathematical model

The dynamic model in Liu and Tang [31] consists of eight state variables. These state variables are defined as follows:

x_1 = concentration of plasma glucagon (in moles per liter);

x_2 = concentration of plasma insulin (in moles per liter);

x_3 = intracellular concentration of glucagon (in moles per liter);

x_4 = intracellular concentration of insulin (in moles per liter);

x_5 = concentration of glucagon receptor (in moles per liter);

x_6 = concentration of insulin-bound receptor (in moles per liter);

x_7 = blood concentration of glycogen (in milligrams per liter);

x_8 = blood concentration of glucose (in milligrams per liter).

The model can be naturally divided into three subsystems, each of which is described below.

3.2.1 Insulin and glucagon transition subsystem

This subsystem governs x_1 and x_2. The dynamics for x_1 are given by

$$\frac{dx_1}{dt} = -(k^p_{1,1} + k^p_{1,2})x_1 + w_1, \tag{3.1}$$

where $k^p_{1,1}$ is a transition rate, $k^p_{1,2}$ is a degradation rate, and w_1 is the glucagon release rate (GRR) defined by

$$w_1 = \frac{G_m}{1 + b_1 \exp a_1(x_8 - C_5)}. \tag{3.2}$$

Furthermore, the dynamics for x_2 are given by

$$\frac{dx_2}{dt} = -(k^p_{2,1} + k^p_{2,2})x_2 + w_2, \tag{3.3}$$

where $k^p_{2,1}$ is a transition rate, $k^p_{2,2}$ is a degradation rate, and w_2 is the insulin release rate (IRR) defined by

$$w_2 = \frac{R_m}{1 + b_2 \exp a_2(C_1 - x_8)}. \tag{3.4}$$

The fractions w_1 and w_2 in equations (3.1)-(3.4) model the natural feedback control mechanisms in the body. Note that G_m is the maximum glucagon infusion rate, R_m is the maximum insulin infusion rate, and a_1, a_2, b_1, b_2, C_1 and C_5 are positive constants.

3.2.2 Insulin and glucagon receptor binding subsystem

This subsystem governs x_3, x_4, x_5 and x_6. The dynamics for this subsystem are given by

$$\frac{dx_3}{dt} = -k^s_{1,1}x_3(R^0_1 - x_5) - k^s_{1,2}x_3 + \frac{k^p_{1,1}V_p x_1}{V}, \tag{3.5}$$

$$\frac{dx_4}{dt} = -k^s_{2,1}x_4(R^0_2 - x_6) - k^s_{2,2}x_4 + \frac{k^p_{2,1}V_p x_2}{V}, \tag{3.6}$$

$$\frac{dx_5}{dt} = -k^s_{1,1}x_3(R^0_1 - x_5) - k^r_1 x_5, \tag{3.7}$$

$$\frac{dx_6}{dt} = -k^s_{2,1}x_4(R^0_2 - x_6) - k^r_2 x_6, \tag{3.8}$$

where $k^s_{1,1}$ and $k^s_{2,1}$ are the hormone-receptor association rates, $k^s_{1,2}$ and $k^s_{2,2}$ are the degradation rates, R^0_1 and R^0_2 are the total concentrations of receptors, k^r_1 and k^r_2 are the inactivation rates, V_p is the plasma insulin volume, and V is the cellular insulin volume.

3.2.3 Glucose production and utilization subsystem

This subsystem governs x_7 and x_8. The dynamics for x_7 are given by

$$\frac{dx_7}{dt} = f_4 - f_5, \tag{3.9}$$

where

$$f_4 = \frac{k_1 x_6}{1 + k_2 x_5} \cdot \frac{V_{\max}^{gs} x_8}{k_m^{gs} + x_8}, \tag{3.10}$$

$$f_5 = k_3 x_5 \frac{V_{\max}^{gp} x_7}{k_m^{gp} + x_7}. \tag{3.11}$$

Here, k_1, k_2 and k_3 are the feedback control gains, $V_{\max}^{gs}$ is the maximum velocity of glycogen phosphorylase, $V_{\max}^{gp}$ is the maximum velocity of glycogen synthase, and k_m^{gs} and k_m^{gp} are the Michaelis-Menton constants.

The dynamics for x_8 are given by

$$\frac{dx_8}{dt} = -f_4 + f_5 - f_1 - f_2 f_3 + G, \tag{3.12}$$

where

$$f_1 = U_b \left(1 - \exp\left(-\frac{x_8}{C_2}\right)\right), \tag{3.13}$$

$$f_2 = \frac{x_8}{C_3}, \tag{3.14}$$

$$f_3 = U_0 + \frac{(U_m - U_0) x_4^{\beta}}{C_4^{\beta} + x_4^{\beta}}. \tag{3.15}$$

Note that U_0, U_b, U_m, C_2, C_3, C_4 and β are positive constants, and G is the exogenous glucose intake derived from digesting food. Here G is expressed using a piecewise linear interpolation of the data in Table 3.1 and plotted in Figure 3.1, with the precise expression given by

$$G = \frac{(g_i - g_{i-1})(t - t_{i-1})}{t - t_{i-1}} + g_{i-1}, \quad t \in [t_{i-1}, t_i], \quad i = 1, \ldots, 11. \tag{3.16}$$

3.2.4 Initial conditions and model constants

We assume that the system is modelled over a 9 hour period, i.e., $t \in [0, 540]$, where t is the time in minutes. The initial conditions prescribed for the model in Liu and Tang [31]

Parameter	Value	Critical points	Value
g_0	0	t_0	0
g_1	69.5950045	t_1	60
g_2	69.2845842	t_2	90
g_3	77.4619058	t_3	120
g_4	83.7348629	t_4	150
g_5	85.7457293	t_5	180
g_6	89.2449716	t_6	240
g_7	87.1436913	t_7	300
g_8	72.9876913	t_8	360
g_9	52.7402225	t_9	420
g_{10}	37.6143743	t_{10}	480
g_{11}	30.2992243	t_{11}	540

Table 3.1: Parameter values for the exogenous glucose input rate G

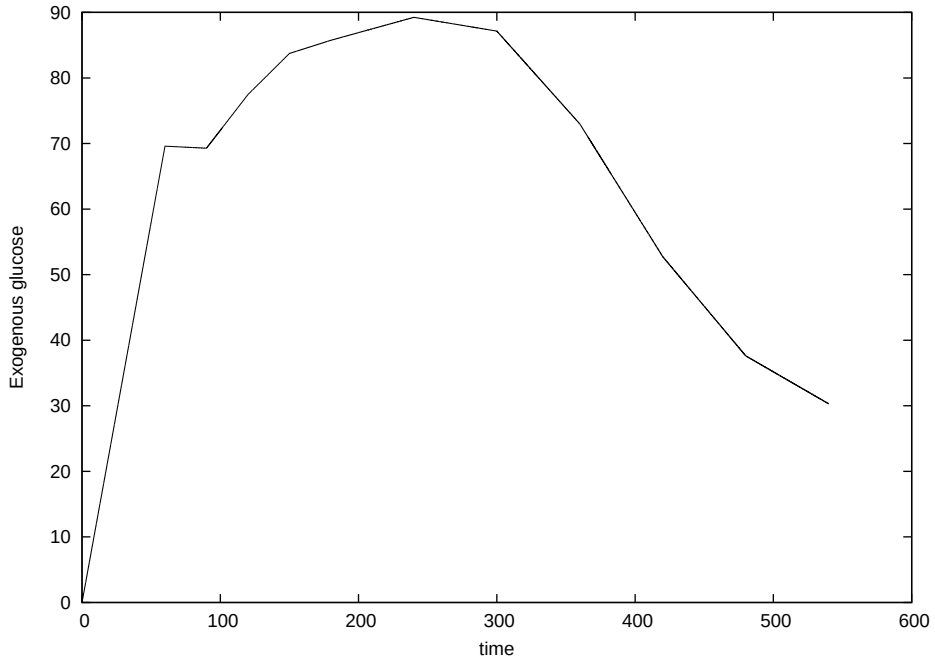

Figure 3.1: Exogenous glucose input rate from the experimental data of Korach-André et al. [27]

are

$$x_1(0) = 1.4 \times 10^{-11}, \tag{3.17}$$
$$x_2(0) = 2 \times 6.945 \times 10^{-12}, \tag{3.18}$$
$$x_3(0) = 0, \tag{3.19}$$
$$x_4(0) = 0.01 \times 6.945 \times 10^{-12}, \tag{3.20}$$
$$x_5(0) = 0, \tag{3.21}$$
$$x_6(0) = 0, \tag{3.22}$$
$$x_7(0) = 200, \tag{3.23}$$
$$x_8(0) = 918. \tag{3.24}$$

The complete model defined by equations (3.1)-(3.24) includes 36 model constants as listed in Table 3.2. Although Liu and Tang [31] give explicit values for each of these constants, they also acknowledge that many of these values are merely informed guesses, usually based on biological understanding or adopted from other publications. In Table 3.2, we have indicated which of the constants are well-defined and which have some uncertainty as to their true values. Note that the values of some of the constants in Table 3.2 differ from the original definitions given by Liu and Tang in [31]. These changes were made based on the advice received via personal communication with Liu and Tang. In particular, we have changed the units of measurement for the parameters $k^s_{2,1}$, R^0_2, C_4, R_m and k_1, and we also use different values for k_i, $i = 1, 2, 3$. These new values are reported in Table 3.2. In addition, Liu and Tang gave the following guidance on the behaviour of some of the uncertain parameters: the degradation rates of glucagon and its receptor ($k^s_{1,2}$, k^r_1) can be assumed to be the same as the respective rates for insulin ($k^s_{2,2}$, k^r_2); the maximum glucagon infusion rate G_m should be selected to be much smaller than R_m; a_1 and b_1 should be selected so that the glucagon secretion w_1 increases rapidly when the blood glucose level x_8 drops to around 800 mg/l; $k^p_{2,1}$ can be assumed to be the same as $k^p_{1,1}$.

3.3 Parameter estimation

Our goal in this chapter is to optimize the model parameters in (3.1)-(3.24), so that the model matches experimental data as closely as possible. As in Liu and Tang [31], we use the experimental data reported in Korach-André et al. [27]. This data set consists of blood glucose measurements from a healthy individual taken after meals. We denote this data set by $\{(\tau_i, \hat{x}^i_8)\}^9_{i=1}$, where τ_i denotes the i-th observation time and $\hat{x}^i_8$ denotes the blood glucose concentration observed at the i-th observation time. The experimental

Constant	Value	Unit	Status
$k^p_{1,1}$	0.14	min^{-1}	uncertain
$k^p_{2,1}$	0.14	min^{-1}	uncertain
$k^p_{1,2}$	0.3	min^{-1}	well-defined
$k^p_{2,2}$	1/6	min^{-1}	uncertain
$k^s_{1,1}$	6×10^7	$\text{M}^{-1}\ \text{min}^{-1}$	well-defined
$k^s_{2,1}$	6×10^7	$\text{M}^{-1}\ \text{min}^{-1}$	well-defined
$k^s_{1,2}$	0.01	min^{-1}	uncertain
$k^s_{2,2}$	0.01	min^{-1}	uncertain
k^r_1	0.2	min^{-1}	uncertain
k^r_2	0.2	min^{-1}	well-defined
R^0_1	9×10^{-13}	M	well-defined
R^0_2	3.6114×10^{-12}	M	well-defined
$v^{gp}_{\max}$	80	mg/l/min	uncertain
k^{gp}_m	600	mg/l	well-defined
$v^{gs}_{\max}$	3.87×10^{-4}	mg/l/min	uncertain
k^{gs}_m	67	mg/l	well-defined
k_1	$2.76900924 \times 10^{11}$	M^{-1}	well-defined
k_2	1.1111111×10^{14}	M^{-1}	well-defined
k_3	1.1111111×10^{12}	M^{-1}	well-defined
V	11	l	uncertain
V_p	3	l	uncertain
U_b	7.2	mg/l/min	uncertain
U_0	4	mg/l/min	uncertain
U_m	94	mg/l/min	uncertain
G_m	2.23×10^{-10}	M/min	uncertain
R_m	4.8615×10^{-10}	M/min	uncertain
C_1	2000	mg/l	uncertain
C_2	144	mg/l	uncertain
C_3	1000	mg/l	uncertain
C_4	5.556×10^{-10}	M/l	uncertain
C_5	1000	mg/l	uncertain
β	1.77	-	uncertain
a_1	0.005	$(\text{mg/l})^{-1}$	uncertain
a_2	1/300	$(\text{mg/l})^{-1}$	uncertain
b_1	10	-	uncertain
b_2	1	-	uncertain

Table 3.2: Constants in the dynamic model (3.1)-(3.24), where M denotes moles.

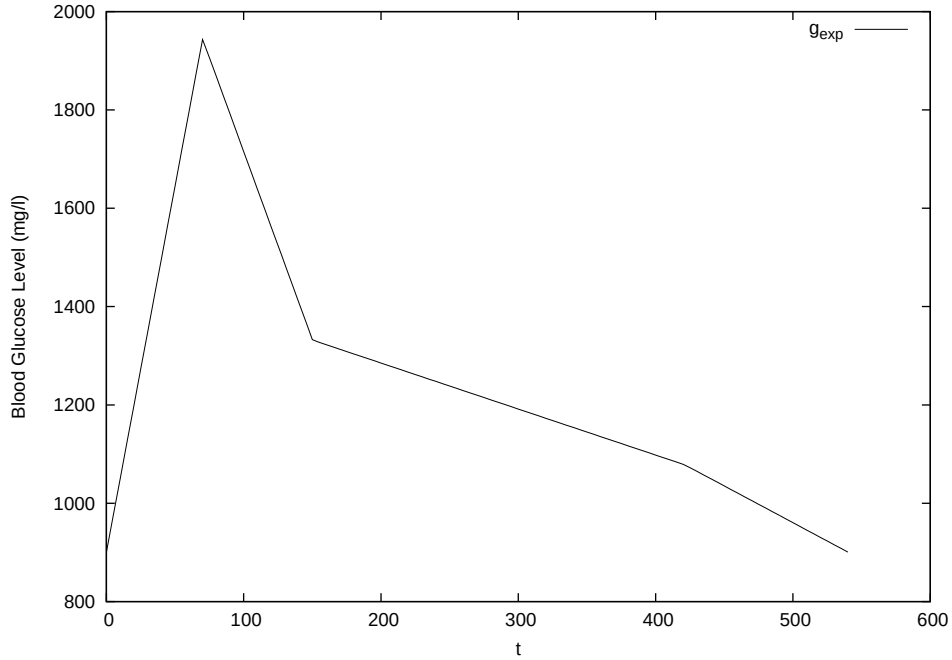

Figure 3.2: Experimental data from Korach-André et al. [27]

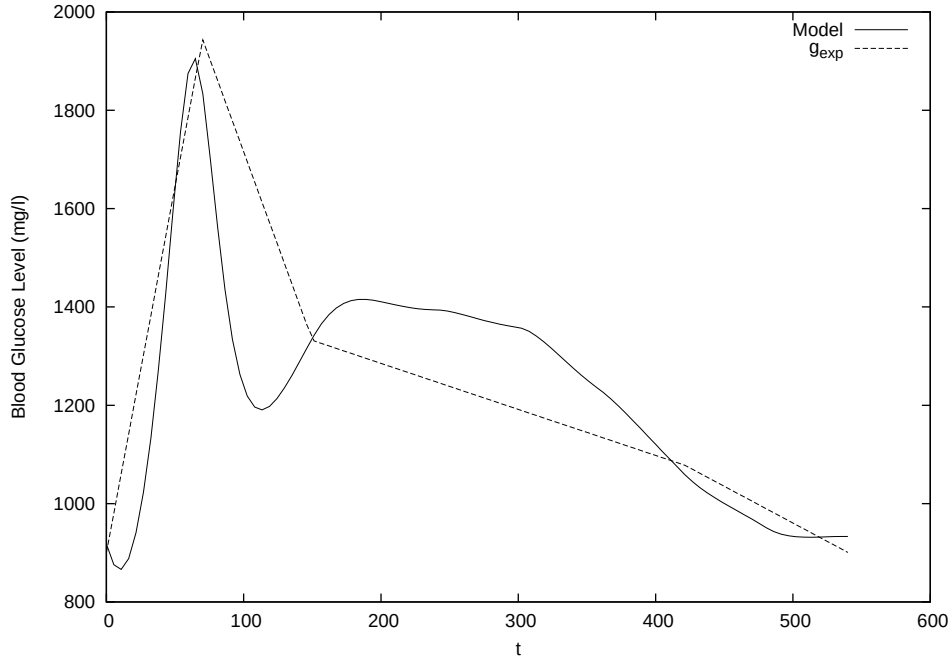

Figure 3.3: Comparison of two blood glucose trajectories: the solid trajectory is the simulated trajectory from (3.1)-(3.24) using the parameter values in Liu and Tang [31]; the dashed trajectory is the experimental data from Korach-André et al. [27]

i	1	2	3	4	5	6	7	8	9
τ_i	0	60	120	150	180	240	380	420	540
$\hat{x}_8^i$	900	1785.29	1530.27	1330.88	1300.55	1244.95	1113.53	1078.2	900.72

Table 3.3: Experimental data from Korach-André et al. [27]

data is shown in Figure 3.2 and listed in Table 3.3. We assume that the experimental data can be interpolated linearly as shown in Figure 3.2 to yield the function $g_{exp}(t)$. Using the original parameter values in Liu and Tang [31], the resulting trajectory for the blood glucose history is shown in Figure 3.3. We will improve the Liu-Tang model by formulating an optimal parameter selection problem to find more appropriate values for the uncertain model parameters in Table 3.2. In the context of Chapter 1, a pure optimal parameter selection problem takes the general form of Problem P_3, but involving only system parameters and no control functions. In other words, each uncertain model parameter in Table 3.2 is associated with a component of the vector of system parameters, z. To cast the problem into the form of P_3, we need to specify the set of feasible system parameters, $\mathcal{Z}$. To do this, for each uncertain parameter, we need to specify upper and lower bounds. For parameters V, U_b, U_0 and β, appropriate bounds were suggested by Liu and Tang [31] in our personal correspondence as shown in Table 3.4. For the other parameters, we use an iterative approach as follows. We initially guess the lower and upper bounds on the basis of the parameter values given in Liu and Tang [31] and solve the resulting parameter estimation problem. Then, for those parameters whose optimal value turns out to be equal to the lower or upper bound, we decreased or increased the respective bound by 10 percent and solved the resulting problem again. This process continues until all optimal parameter values are contained in the interior of their respective bound intervals. This iterative approach is necessary because the model (3.1)-(3.24) is quite sensitive to some of the model parameters. It is difficult to integrate the dynamics numerically when the parameter values are too far from those in the previous stage.

For the purpose of model matching, we consider three possible objectives and solve the resulting parameter estimation problems with MISER3.3.

3.3.1 Case 1

In this case, our aim is to match the simulated blood glucose level to the experimental data $g_{exp}(t)$ over the entire time horizon. Thus, the aim is to determine values of the uncertain parameters so as to minimize

$$J_1 = \int_0^{540} \left(x_8(t) - g_{exp}(t)\right)^2 dt \tag{3.25}$$

Parameter	Lower bound	Upper bound
V	10	25
U_b	4	12
U_0	4	12
β	1	2

Table 3.4: Lower and upper bounds for V, U_b, U_0, and β

subject to the dynamic model defined by equations (3.1)-(3.24).

The resulting optimal values of the uncertain parameters are shown in Table 3.5 and the glucose trajectory generated from (3.1)-(3.24) using these optimal values is shown in Figure 3.4. Comparing Figures 3.3 and 3.4, it is clear that the optimal parameter values yield significant improvements in model matching. However, there appears to be some mismatch between the model trajectory and experimental data at the terminal time. Hence, we consider a modified version of the objective function (3.25) in the next case.

3.3.2 Case 2

Here, we add another term to the objective function that measures the difference between the predicted and actual blood glucose levels at the terminal time. Specifically, the aim is to minimize

$$J_2 = w\left(x_8(540) - 900.72\right)^2 + \int_0^{540} \left(x_8(t) - g_{exp}(t)\right)^2 dt \tag{3.26}$$

subject to the dynamics (3.1)-(3.24), where the weight w is chosen as $w = 1000$. The idea here is to force better agreement between the model output and the experimental data at the end of the time horizon. The resulting optimal values for the uncertain model parameters are shown in Table 3.5. As seen from the resulting optimal glucose trajectory in Figure 3.5, a closer match of the trajectories at the terminal time can be achieved at the expense of increased error earlier in the time horizon.

3.3.3 Case 3

Since the experimental data in Table 3.3 is only measured at a small number of isolated times, the actual glucose level between these times is unknown. Thus, our definition of $g_{exp}(t)$ as a piecewise linear interpolating function and the use of the integral terms in (3.25) and (3.26) may not be appropriate. An alternative parameter estimation problem

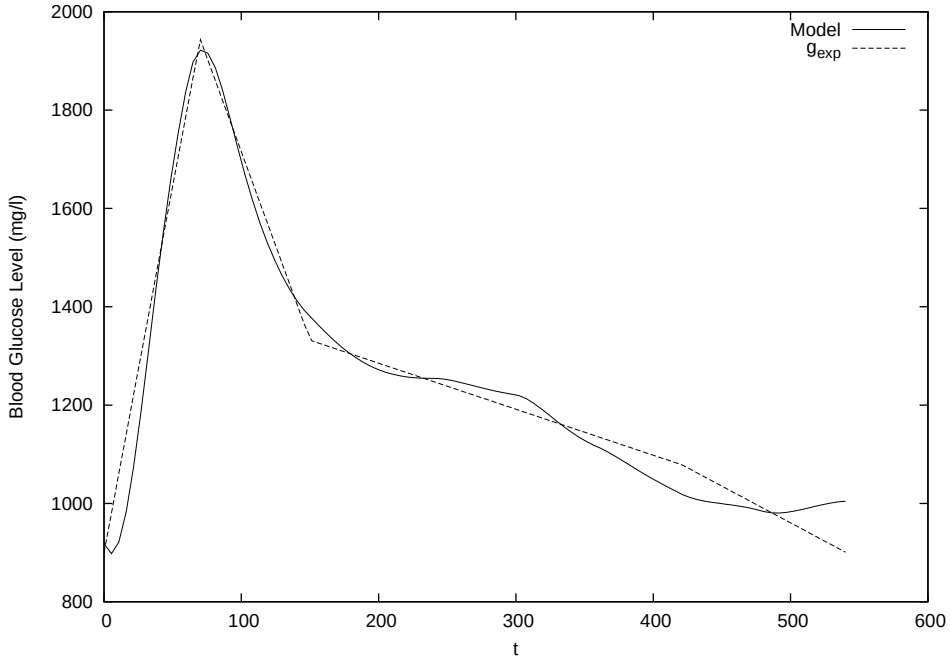

Figure 3.4: Comparison of two blood glucose trajectories: the solid trajectory is the simulated trajectory from (3.1)-(3.24) using the optimal parameter values for Case 1; the dashed trajectory is the experimental data from Korach-André et al. [27]

is to choose values for the uncertain model parameters in order to minimize

$$J_3 = \sum_{i=1}^{9} \left(x_8(\tau_i) - \hat{x}_8^i \right)^2 \tag{3.27}$$

subject to the dynamics (3.1)-(3.24), where $\hat{x}_8^i$ and τ_i, $i = 1, \ldots, 9$, are as defined in Table 3.3. Note that this objective function is not in the standard canonical form due to the presence of multiple non-integral terms that depend on the state at intermediate times (called characteristic times in the optimal control literature). Nevertheless, objective functions of this form can be handled using the techniques developed in [34] and [40], which have been incorporated into the MISER3.3 software [25].

The resulting optimal model parameter values are shown in Table 3.5. As can be seen in Figure 3.6, the resulting blood glucose level tracks the individual experimental measurements very closely, although, as expected, it does not follow the interpolating function $g_{exp}(t)$ as closely as we observed for Case 1.

Parameter	**Original value**	**Case 1**	**Case 2**	**Case 3**
$k^p_{1,1}$	0.14	1.28929	2.19177	1.37664
$k^p_{2,1}$	0.14	0.100804	0.114719	0.154412
$k^p_{1,2}$	0.3	0.3	0.3	0.3
$k^p_{2,2}$	1/6	0.437605	0.743780	0.743944
$k^s_{1,1}$	6×10^7	6×10^7	6×10^7	6×10^7
$k^s_{2,1}$	6×10^7	6×10^7	6×10^7	6×10^7
$k^s_{1,2}$	0.01	7.19985×10^{-3}	2.16×10^{-3}	7.6107×10^{-2}
$k^s_{2,2}$	0.01	9.52782×10^{-3}	8.5×10^{-3}	8.95549×10^{-3}
k^r_1	0.2	2.59194×10^{-2}	7.776×10^{-3}	2.4×10^{-1}
k^r_2	0.2	0.2	0.2	0.2
R^0_1	9×10^{-13}	9×10^{-13}	9×10^{-13}	9×10^{-13}
R^0_2	3.6114×10^{-12}	3.6114×10^{-12}	3.6114×10^{-12}	3.6114×10^{-12}
$v^{gp}_{\max}$	80	25.0197	24.6129	24.7160
k^{gp}_m	600	600	600	600
$v^{gs}_{\max}$	3.87×10^{-4}	3.41805×10^{-3}	5.811×10^{-3}	5.811×10^{-3}
k^{gs}_m	67	67	67	67
k_1	2.76901×10^{11}	2.76901×10^{11}	2.76901×10^{11}	2.76901×10^{11}
k_2	1.11111×10^{14}	1.11111×10^{14}	1.11111×10^{14}	1.11111×10^{14}
k_3	1.11111×10^{12}	1.11111×10^{12}	1.11111×10^{12}	1.11111×10^{12}
V	11	10.0004	10.3573	10.0181
V_p	3	2.41375	3.44929	2.77484
U_b	7.2	4	4	7.80699
U_0	4	4	4	8.14836
U_m	94	227.508	227.972	227.642
G_m	2.23×10^{-10}	2.05367×10^{-9}	3.49116×10^{-9}	1.87341×10^{-9}
R_m	4.8615×10^{-10}	2.29663×10^{-10}	3.98353×10^{-10}	4.22818×10^{-10}
C_1	2000	1114.19	1114.07	1114.29
C_2	144	345.384	345.434	345.378
C_3	1000	1061.82	1061.77	1061.77
C_4	5.556×10^{-10}	1.9556×10^{-9}	3.32383×10^{-9}	3.28142×10^{-9}
C_5	1000	1124.67	1124.67	1124.68
β	1.77	1.14055	1.17821	1.33999
a_1	0.005	3.48467×10^{-2}	5.9238×10^{-2}	5.9238×10^{-2}
a_2	1/300	1.45946×10^{-2}	8.59508×10^{-3}	8.70603×10^{-3}
b_1	10	11.4710	11.4664	11.4667
b_2	1	1.15002	1.1893	1.955

Table 3.5: Comparing the optimized parameter values with the values in [31]

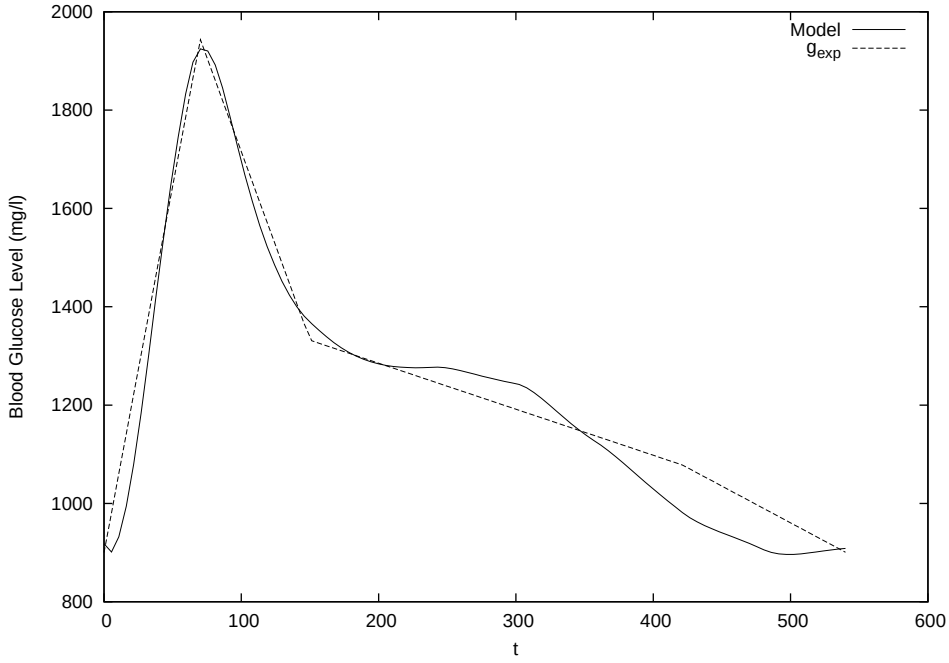

Figure 3.5: Comparison of two blood glucose trajectories: the solid trajectory is the simulated trajectory from (3.1)-(3.24) using the optimal parameter values for Case 2; the dashed trajectory is the experimental data from Korach-André et al. [27]

3.4 Model sensitivity

In Liu and Tang [31], a sensitivity test was performed by doubling and halving the insulin feedback rate and observing the corresponding model response. For comparison, we perform the same sensitivity test on the model with the optimized parameters from Case 1. This involves replacing the original insulin feedback rate w_2 in (3.4) by

$$w_2 = \frac{2R_m}{1 + b_2 \exp a_2(C_1 - x_8)}, \tag{3.28}$$

and

$$w_2 = \frac{\frac{1}{2}R_m}{1 + b_2 \exp a_2(C_1 - x_8)}, \tag{3.29}$$

respectively. The resulting blood glucose levels are shown in Figures 3.7 and 3.8, respectively. Compared to the corresponding figures in Liu and Tang [31], the glucose levels in Figures 3.7 and 3.8 are further away from the experimental measurements. This is expected, since optimizing the model parameters will generally lead to a more sensitive model. Also, these results agree with the intuitive understanding of the blood glucose regulatory system in terms of the effects of changing insulin levels.

While we do not pursue this option here, note that it is possible to formulate a modi-

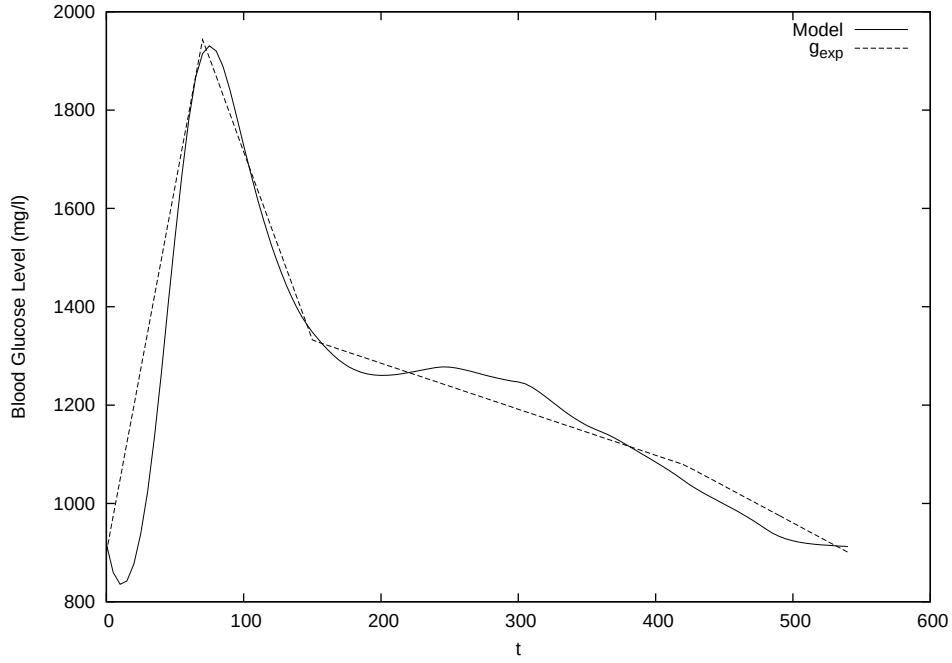

Figure 3.6: Comparison of two blood glucose trajectories: the solid trajectory is the simulated trajectory from (3.1)-(3.24) using the optimal parameter values for Case 3; the dashed trajectory is the experimental data from Korach-André et al. [27]

fied optimal parameter selection problem where part of the objective is to minimize the sensitivity of the model with respect to various disturbances of the type considered here. See [33] for details.

3.5 Optimal insulin and glucose release rates

The feedback controls (3.2) and (3.4) model the physiology of the pancreas. Liu and Tang [31] have suggested that these natural feedback controls may not be "optimal" in the sense of regulating the blood glucose level. They formulated a quadratic optimal control problem which seeks to find the corresponding optimal open loop controls but were not able to solve this problem. In this section, we demonstrate that the optimal open loop controls for the insulin and glucose release rates can be readily calculated using the MISER3.3 software [25]. We replace the closed loop controls w_1 and w_2 by corresponding open loop controls u_1 and u_2, respectively. Thus, equations (3.1) and (3.3) become, respectively,

$$\frac{dx_1}{dt} = -(k^p_{1,1} + k^p_{1,2})x_1 + u_1, \tag{3.30}$$

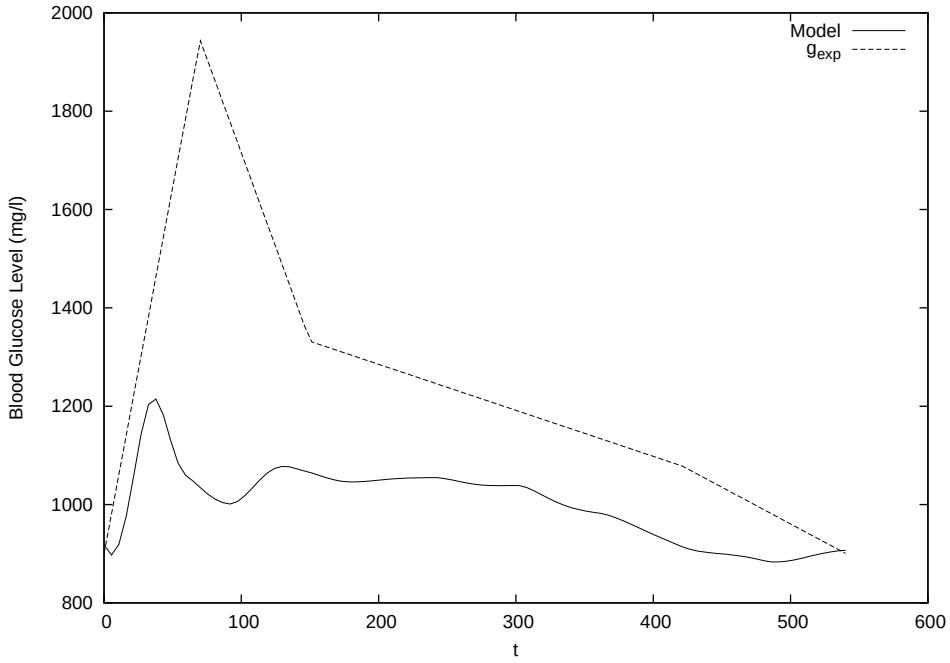

Figure 3.7: Blood glucose level when w_2 is defined by (3.28).

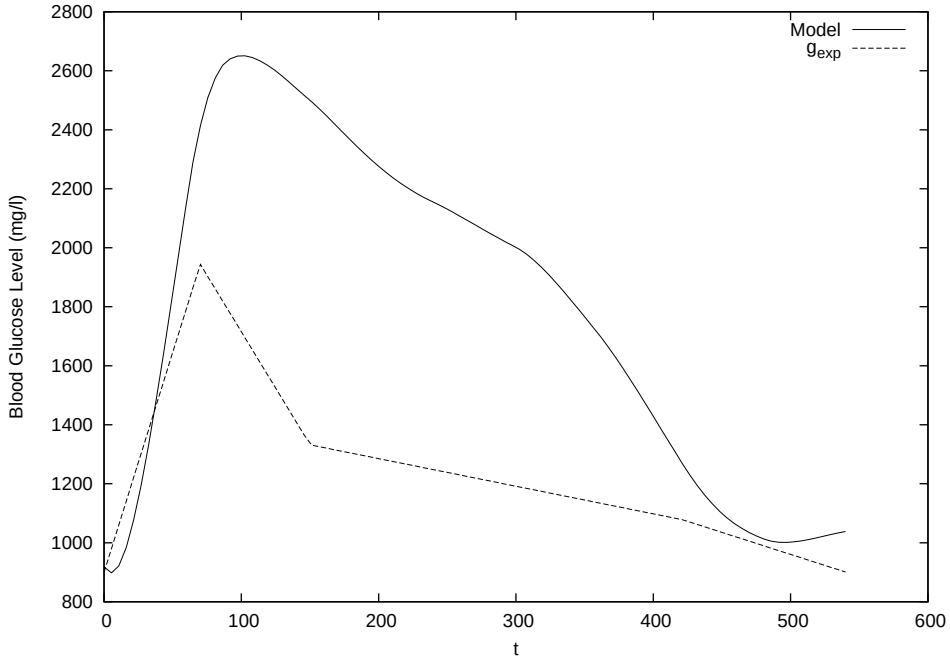

Figure 3.8: Blood glucose level when w_2 is defined by (3.29).

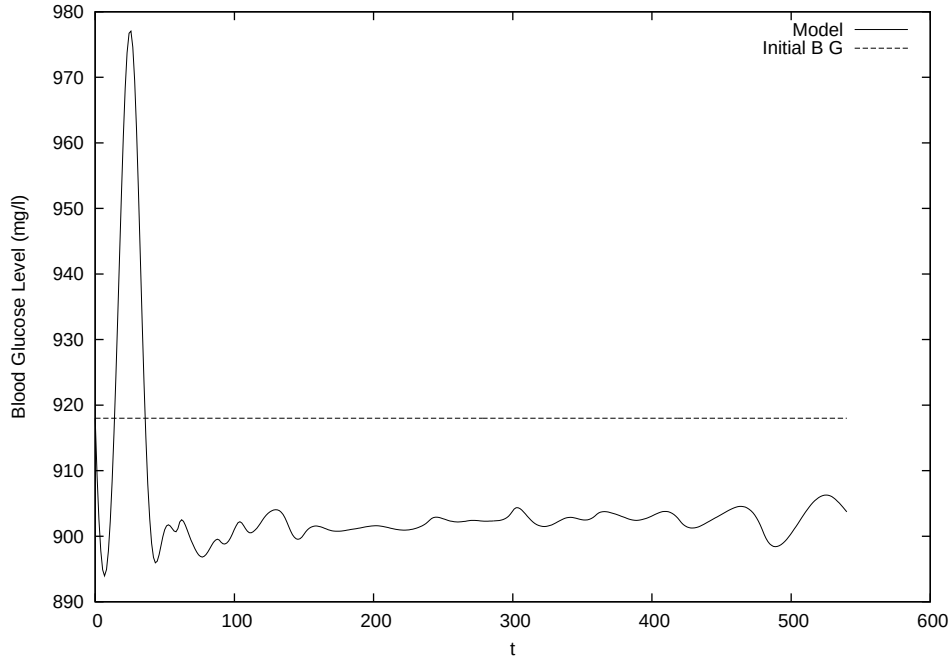

Figure 3.9: Optimal blood glucose trajectory corresponding to the optimal solution in Section 3.5.

and

$$\frac{dx_2}{dt} = -(k_{2,1}^p + k_{2,2}^p)x_2 + u_2. \tag{3.31}$$

We assume that both u_1 and u_2 are parameterized as piecewise linear continuous functions in accordance with the control parameterization method ([30], [55]). The objective function (adopted from the suggestion in [31]) is given by:

$$J = \int_0^{540} \{(x_8(t) - 918)^2 + u_1^2(t) + u_2^2(t)\}dt. \tag{3.32}$$

This objective function penalizes both control expenditure and blood glucose deviation from the initial level. The problem is to minimize (3.32) subject to the dynamic model (3.1)-(3.24) with the optimized parameters from Case 1 (and with (3.1) and (3.3) replaced by (3.30) and (3.31)). As the model is quite sensitive to changes in u_1 and u_2, we use a homotopy approach with the initial guesses of u_1 and u_2 as w_1 and w_2 (from the Case 1 optimized the model), respectively. We initially imposed tight lower and upper bounds on u_1 and u_2 around the initial guesses. These bounds were then slowly relaxed over a series of optimization iterations until no more improvement in the objective was observed.

The optimal blood glucose trajectory is shown in Figure 3.9 and the optimal controls are shown in Figures 3.10 and 3.11. As can be seen from Figure 3.9, the blood glucose level corresponding to the optimal open loop controls remains very close to the initial

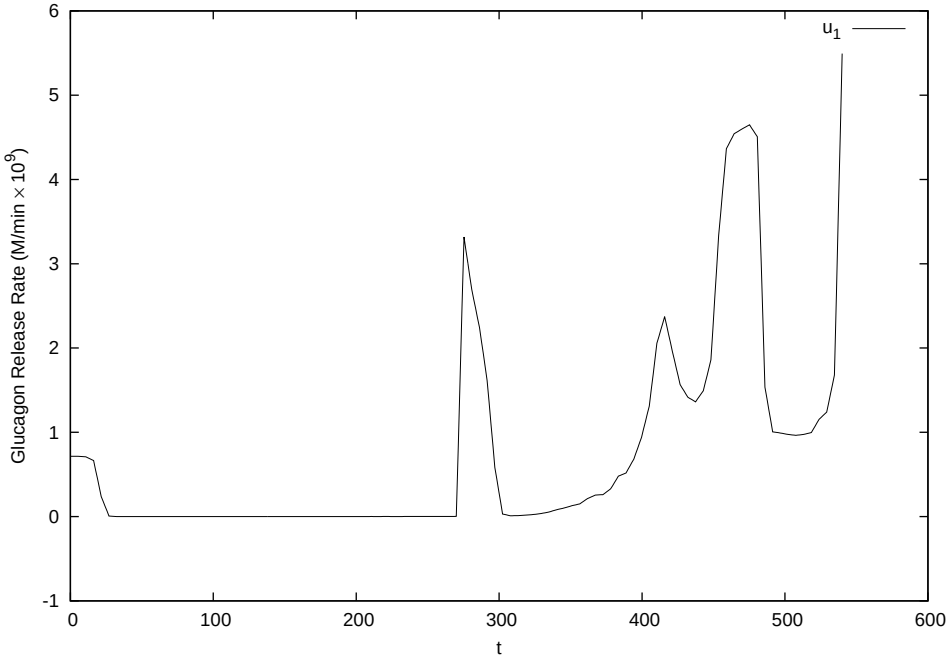

Figure 3.10: The optimal glucagon release rate.

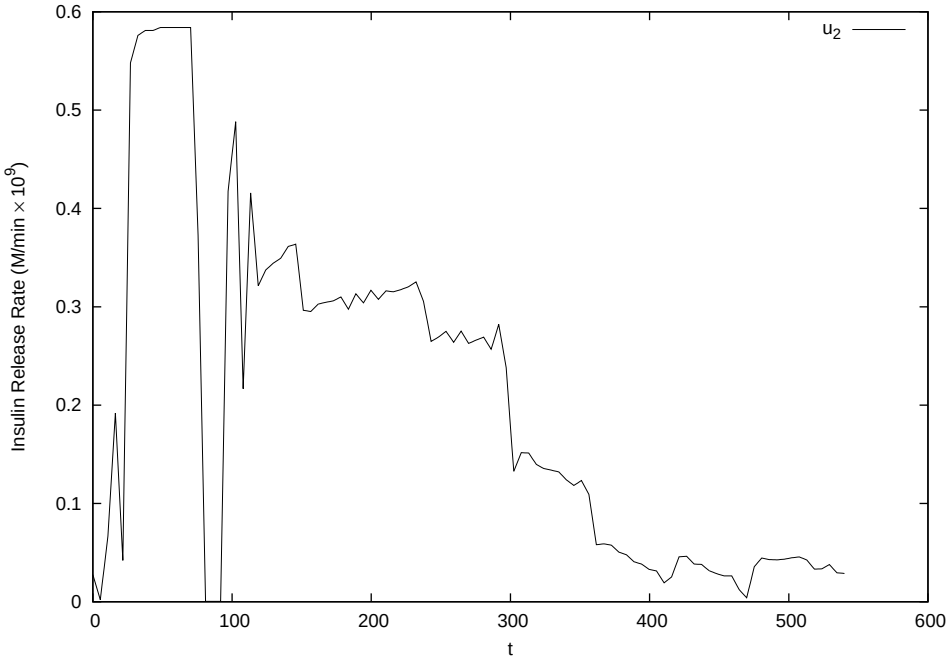

Figure 3.11: The optimal insulin release rate.

blood glucose level (918 mg/l= 5.1 mmol/l) over the entire time horizon. This clearly demonstrates that excellent glucose control is achievable with the open loop formulation. Note that this is a purely theoretical study to determine whether open loop blood glucose control is possible and what the corresponding controls look like. In practice, delivery of glucagon or insulin in this manner is not practical. However, the blood glucose response is quite different from that observed in experimental results. This raises the question of why the blood glucose regulatory system in the human body does not follow the 'optimal' approach calculated via the open loop formulation. One should note that the glucose regulatory system forms only one part of a more complex metabolic system that controls the human body. There are probably sound reasons why elevated blood glucose levels occur in humans after the ingestion of a meal, but these are not reflected in the glucose regulatory model considered here.

3.6 Conclusions

We have solved a complex model matching problem in which a glucose regulatory model must be fitted to experimental data to minimize total modelling error. We investigated several different model matching objectives and found that significant improvement in matching the model to experimental data was achieved in all cases when compared to the results in Liu and Tang [31]. It is difficult for us to judge the relative merits of these objectives and the ultimate choice is best left to experts who are more familiar with the use of the model in relation to the real physical system. Nevertheless, we have demonstrated that the proposed model matching strategy yields very good results in this scenario and it should be used more widely for other biological systems.

As expected, we also found that the optimized model was more sensitive to changes in the insulin release rate. Finally, we showed that open loop optimal controls can be readily calculated for the glucose regulatory system. The resulting glucose profiles do not match real profiles observed experimentally, which suggests that there may be other mechanisms at play in the real system which are not accounted for in the mathematical model.

Future work will consider the implementation of the glucose regulatory model for diabetic individuals and how their conditions can be controlled optimally.

CHAPTER 4

Insulin Injection and Exercise Scheduling for Diabetics: An Optimal Control Model

In this chapter, we develop a composite dynamic model for simulating the effects of exercise and subcutaneous insulin injections on the blood glucose regulatory system. This model consists of 12 state variables naturally divided into four subsystems—the glucagon and insulin transition subsystem, the receptor binding subsystem, the glucose subsystem and the exercise subsystem—with dynamic system switches at the insulin injection times. We formulate an optimal control problem in which the aim is to determine optimal injection times, optimal injection volumes and optimal exercise regimes to regulate the blood glucose level. A numerical approach, based on control parameterization and the time scaling transform, is then developed for solving the optimal control problem. Numerical results for a series of five scenarios show that optimal treatment regimes can be readily determined via the proposed approach. Good blood glucose can be achieved given moderate levels of treatment.

4.1 Introduction

Insulin was first isolated and purified as a treatment for diabetes in 1920. However, a permanent cure has been elusive until this day. Type 1 diabetes is managed through the use of analogue insulin as well as targeted diet and exercise. Type 2 diabetes treatment may start with non-insulin medication, which stimulates the body's own insulin generation or reduces insulin resistance. A controlled diet may be sufficient to treat very early cases of type 2 diabetes. However, as the disease progresses, insulin treatment will eventually be required. Moreover, due to issues such as age, excessive weight and high blood pressure, the level of exercise may be restricted for some patients, especially if they have other health problems such as heart disease and risk of strokes.

The three most common methods for administering insulin are the intra-peritoneal, subcutaneous (SC) and intravenous (IV) injections [12]. SC injection is the most common

method and involves either direct injection at the site, or injection via an external insulin pump, which provides a steady stream of insulin throughout the day. On the other hand, medical supervision is required to receive IV insulin injections via veins and surgical administration is required to implant an insulin pump in the peritoneum (the serous membrane lining the walls of the abdominal and pelvic cavities (parietal peritoneum)) in order to deliver intra-peritoneal insulin. In addition, SC injections are a less expensive method for patients to receive their daily injections. Thus, in this chapter, we focus on the subcutaneous injection method. Many factors can affect the insulin absorption process such as temperature, insulin concentration and volume and injection site and depth. In addition, the insulin state can be hexameric, dimeric or monomeric which affects the time taken for the insulin preparation to be absorbed into blood plasma. We review several mathematical models of insulin absorption and choose one suitable for incorporation into the existing model.

In this chapter, we extend the mathematical model of the human blood glucose regulatory system originally proposed by Liu and Tang [31]. Specifically, we focus on creating a more complete model that captures the effect of exercise and subcutaneous insulin injections on the blood glucose level for diabetic individuals. Based on the composite model, we formulate an optimal control problem which seeks to minimize the difference between the blood glucose level for a diabetic individual and a desired trajectory. To generate accurate values for the optimal insulin injection times, we apply a time scaling transformation technique ([30], [34]). Numerical results show that, on the basis of these formulations, good blood glucose control can be readily achieved for a variety of desired blood glucose trajectories with the use of the MISER3.3 optimal control software [25].

This chapter is organized as follows. We first review the model described in [31] and [3] in Section 4.2. Then, in Section 4.3, we propose extensions of the model in Section 4.2 which take into account the effects of both insulin injections and exercise. In Section 4.4, we formulate a combined optimal control and optimal parameter selection problem with the aim of following a desired blood glucose profile as closely as possible. In order to allow for the numerical optimization of the injection times, we adopt the control parameterization and time scaling transformation methods described in Chapter 1. We then solve the transformed problem for a variety of scenarios using the optimal control software MISER3.3. [25] in Section 4.5. Finally, we conclude the chapter with a discussion of the numerical results and suggestions for future work.

4.2 Original model

We review once more the dynamic model in Liu and Tang [31] consisting of eight state variables. These state variables are defined as follows:

x_1 = concentration of plasma glucagon (in moles per liter);

x_2 = concentration of plasma insulin (in moles per liter);

x_3 = intracellular concentration of glucagon (in moles per liter);

x_4 = intracellular concentration of insulin (in moles per liter);

x_5 = concentration of glucagon receptor (in moles per liter);

x_6 = concentration of insulin-bound receptor (in moles per liter);

x_7 = blood concentration of glycogen (in milligrams per liter);

x_8 = blood concentration of glucose (in milligrams per liter).

The model can be naturally divided into three subsystems, as described in the following subsections (see [31] and [3] for more details).

4.2.1 Insulin and glucagon transition subsystem

This subsystem governs state variables x_1 and x_2. The dynamics for x_1 are given by

$$\frac{dx_1}{dt} = -(k^p_{1,1} + k^p_{1,2})x_1 + w_1, \tag{4.1}$$

where $k^p_{1,1}$ is a transition rate, $k^p_{1,2}$ is a degradation rate, and w_1 is the glucagon release rate (GRR) defined by

$$w_1 = \frac{G_m}{1 + b_1 \exp a_1(x_8 - C_5)}. \tag{4.2}$$

The dynamics for x_2 are given by

$$\frac{dx_2}{dt} = -(k^p_{2,1} + k^p_{2,2})x_2 + w_2, \tag{4.3}$$

where $k^p_{2,1}$ is a transition rate, $k^p_{2,2}$ is a degradation rate, and w_2 is the insulin release rate (IRR) defined by

$$w_2 = \frac{R_m}{1 + b_2 \exp a_2(C_1 - x_8)}. \tag{4.4}$$

The fractions w_1 and w_2 in equations (4.1)-(4.4) model the natural feedback control mechanisms in the body. Note that G_m is the maximum glucagon infusion rate, R_m is the maximum insulin infusion rate, and a_1, a_2, b_1, b_2, C_1 and C_5 are positive constants.

4.2.2 Insulin and glucagon receptor binding subsystem

This subsystem governs state variables x_3, x_4, x_5 and x_6. The dynamics for this subsystem are given by

$$\frac{dx_3}{dt} = -k^s_{1,1}x_3(R^0_1 - x_5) - k^s_{1,2}x_3 + \frac{k^p_{1,1}V_p x_1}{V}, \tag{4.5}$$

$$\frac{dx_4}{dt} = -k^s_{2,1}x_4(R^0_2 - x_6) - k^s_{2,2}x_4 + \frac{k^p_{2,1}V_p x_2}{V}, \tag{4.6}$$

$$\frac{dx_5}{dt} = -k^s_{1,1}x_3(R^0_1 - x_5) - k^r_1 x_5, \tag{4.7}$$

$$\frac{dx_6}{dt} = -k^s_{2,1}x_4(R^0_2 - x_6) - k^r_2 x_6, \tag{4.8}$$

where $k^s_{1,1}$ and $k^s_{2,1}$ are the hormone-receptor association rates, $k^s_{1,2}$ and $k^s_{2,2}$ are the degradation rates, R^0_1 and R^0_2 are the total concentrations of receptors, k^r_1 and k^r_2 are the inactivation rates, V_p is the plasma insulin volume, and V is the cellular insulin volume.

4.2.3 Glucose production and utilization subsystem

This subsystem governs state variables x_7 and x_8. The dynamics for x_7 are given by

$$\frac{dx_7}{dt} = f_4 - f_5, \tag{4.9}$$

where

$$f_4 = \frac{k_1 x_6}{1 + k_2 x_5} \cdot \frac{V^{gs}_{\max} x_8}{k^{gs}_m + x_8}, \tag{4.10}$$

$$f_5 = k_3 x_5 \frac{V^{gp}_{\max} x_7}{k^{gp}_m + x_7}. \tag{4.11}$$

Here, k_1, k_2 and k_3 are the feedback control gains, $V^{gs}_{\max}$ is the maximum velocity of glycogen phosphorylase, $V^{gp}_{\max}$ is the maximum velocity of glycogen synthase, and k^{gs}_m and k^{gp}_m are Michaelis-Menton constants.

The dynamics for x_8 are given by

$$\frac{dx_8}{dt} = -f_4 + f_5 - f_1 - f_2 f_3 + G, \tag{4.12}$$

where

$$f_1 = U_b \left(1 - \exp\left(-\frac{x_8}{C_2}\right)\right), \tag{4.13}$$

$$f_2 = \frac{x_8}{C_3}, \tag{4.14}$$

$$f_3 = U_0 + \frac{(U_m - U_0)x_4^\beta}{C_4^\beta + x_4^\beta}. \tag{4.15}$$

Here, $U_0, U_b, U_m, C_2, C_3, C_4$ and β are positive constants, and G is the exogenous glucose input rate. As in the earlier chapters, we use the experimental data of Korach-André et al. [27] to define G.

4.2.4 Initial conditions and model constants

We assume that the system is modelled over a 9 hour period, i.e., $t \in [0, 540]$, where t is the time in minutes. The initial conditions prescribed for the model are

$$x_1(0) = 1.4 \times 10^{-11}, \tag{4.16}$$

$$x_2(0) = 2 \times 6.945 \times 10^{-12}, \tag{4.17}$$

$$x_3(0) = 0, \tag{4.18}$$

$$x_4(0) = 0.01 \times 6.945 \times 10^{-12}, \tag{4.19}$$

$$x_5(0) = 0, \tag{4.20}$$

$$x_6(0) = 0, \tag{4.21}$$

$$x_7(0) = 200, \tag{4.22}$$

$$x_8(0) = 918. \tag{4.23}$$

The complete model defined by equations (4.1)-(4.23) includes 36 model constants. In Chapter 3, we formulated an optimal parameter selection problem to optimize these constants, so that the model matches desired blood glucose data from Korach-André et al. [27] as closely as possible. This data set consists of blood glucose measurements from a healthy individual taken after a meal. We denote this data set by $\{(\tau_i, \hat{x}_8^i)\}_{i=1}^9$, where τ_i denotes the i-th observation time and $\hat{x}_8^i$ denotes the blood glucose concentration observed at the i-th observation time. This blood glucose profile is shown in Figure 4.1 and the data points are listed in Table 4.1. We assumed that the experimental data can be interpolated linearly as shown in Figure 4.1 to yield the function $g_{exp}(t)$. A good match between the model and the desired data in [27] was achieved in Chapter 3 and the optimized values of the model constants are listed in Table 4.2.

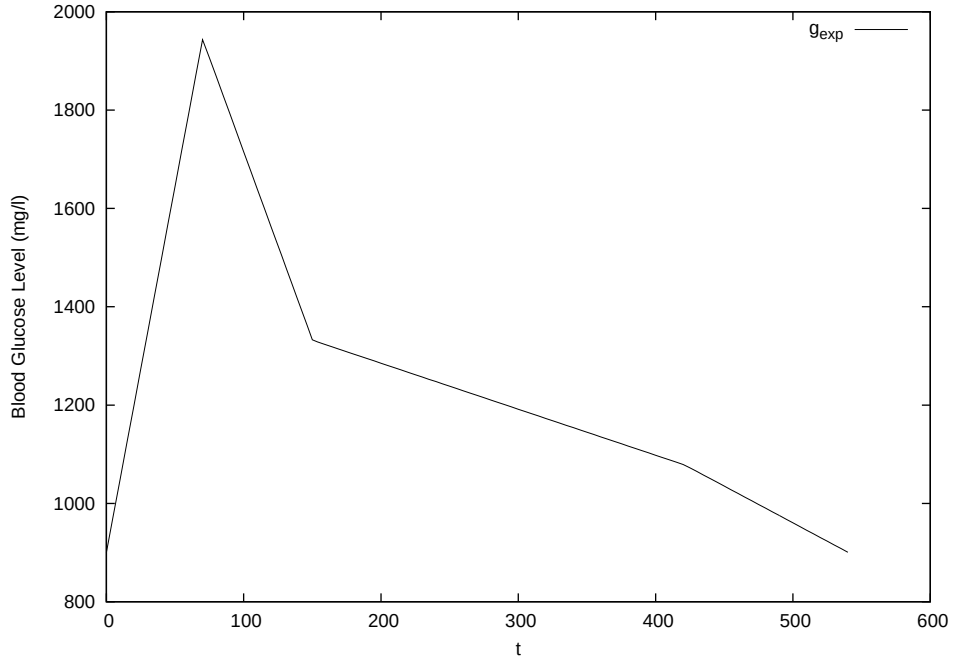

Figure 4.1: The desired blood glucose data from Korach-André et al. [27]

i	1	2	3	4	5	6	7	8	9
τ_i	0	60	120	150	180	240	380	420	540
$\hat{x}_8^i$	900	1785.29	1530.27	1330.88	1300.55	1244.95	1113.53	1078.2	900.72

Table 4.1: The desired data from Korach-André et al. [27]

4.3 New composite model with exercise and insulin injections

To adopt the Liu and Tang model to a diabetic subject, we must assume that the natural insulin release rate defined by equation (4.4) is impaired. For a type 1 diabetic, the maximum insulin release rate should be chosen as $R_m = 0$ in model (4.1)-(4.23). Also, $R_m \in (0, 1)$ can be used to model type 2 diabetics with varying degrees of severity of the condition.

4.3.1 SC injections

A variety of mathematical models for the absorption of insulin from subcutaneous (SC) injections into blood plasma have been proposed in the literature. There is a significant

Constant	Value	Unit
$k^p_{1,1}$	1.28929	min^{-1}
$k^p_{2,1}$	0.100804	min^{-1}
$k^p_{1,2}$	0.3	min^{-1}
$k^p_{2,2}$	0.437605	min^{-1}
$k^s_{1,1}$	6×10^7	$\text{M}^{-1}\ \text{min}^{-1}$
$k^s_{2,1}$	6×10^7	$\text{M}^{-1}\ \text{min}^{-1}$
$k^s_{1,2}$	7.19985×10^{-3}	min^{-1}
$k^s_{2,2}$	9.52782×10^{-3}	min^{-1}
k^r_1	2.59194×10^{-2}	min^{-1}
k^r_2	0.2	min^{-1}
R^0_1	9×10^{-13}	M
R^0_2	3.6114×10^{-12}	M
$v^{gp}_{\max}$	345.384	mg/l/min
k^{gp}_m	600	mg/l
$v^{gs}_{\max}$	3.41805×10^{-3}	mg/l/min
k^{gs}_m	67	mg/l
k_1	2.76901×10^{11}	M^{-1}
k_2	1.1111111×10^{14}	M^{-1}
k_3	1.1111111×10^{12}	M^{-1}
V	10.0004	l
V_p	2.41375	l
U_b	4	mg/l/min
U_0	4	mg/l/min
U_m	227.508	mg/l/min
G_m	2.05367×10^{-9}	M/min
R_m	2.29663×10^{-10}	M/min
C_1	1.11419×10^{-3}	mg/l
C_2	345.384	mg/l
C_3	1061.82	mg/l
C_4	1.9556×10^{-9}	M/l
C_5	1124.67	mg/l
β	1.14055	-
a_1	0.0348467	$(\text{mg/l})^{-1}$
a_2	0.0145946	$(\text{mg/l})^{-1}$
b_1	11.471	-
b_2	1.15002	-

Table 4.2: Optimized values for the model constants

Insulin type	Parameter			
	s	a	b	V_d
Short acting (soluble)	2	4.31965×10^5	102	12×10^{-6}
Intermediate acting (NPH)	2	1.5550756×10^6	294	12×10^{-6}
long acting (ultralente)	2.5	0	780	12×10^{-6}
Unit	-	min/M	min	l

Table 4.3: Berger model parameters for different types of insulin; intermediate, short and long acting insulin

range in the complexity of these models, starting with a simple single pool model involving a delay term to approximate the absorption of fast acting insulin [26]. Trajanski et al. [57] present a far more complex model where the diffusion of insulin from the injection site is approximated via the transition across a series of concentric spherical shells. This leads to a series of partial differential equations and, while accurate results can certainly be achieved, there is a significant computational cost associated with this model. A detailed review of the various absorption models is given in [44]. After careful consideration of the suitability of each of these models for our purposes and, guided by the conclusions in [44], we settled on the model first proposed in Berger et al. [8]. Briefly, in this model the amount of absorbed insulin from the SC injection depot, $A(t)$, is assumed to be given by

$$A(t) = 1 - \frac{t^s}{(T_{50})^s + t^s}, \tag{4.24}$$

where t is the time elapsed since the injection and T_{50} is the duration required to reach a 50% absorption of the injected insulin. This is given by

$$T_{50} = aD + b, \tag{4.25}$$

where D is the insulin dose, and s, a and b are constants which assume different values for different insulin preparations. Table 4.3 shows these parameter values for different types of insulin. The time derivative of $A(t)$, multiplied by the injection dose, then gives the input flux of injected insulin into the plasma,

$$\frac{t^{s-1} s (T_{50})^s D}{V_d((T_{50})^s + t^s)^2}, \tag{4.26}$$

where V_d is the plasma insulin distribution volume.

We now allow for up to M SC insulin injections over the time horizon $[0, T]$. Each one of these has an individual effect on the plasma glucose concentration and this is modelled

by replacing equation (4.3) with

$$\frac{dx_2}{dt} = -(k_{2,1}^p + k_{2,2}^p)x_2 + w_2 + \sum_{i=1}^{M} I_i(t), \tag{4.27}$$

where

$$I_i(t) = \frac{s_i(t-t_i)^{s_i-1}(T_i)^{s_i}D_iH(t-t_i)}{V_d((T_i)^{s_i} + (t-t_i)^{s_i})^2}, \quad i = 1, \ldots, M, \tag{4.28}$$

and $t_i, i = 1, \ldots, M$, are the insulin injection times and H is the Heaviside step function defined by

$$H(t) = \begin{cases} 0, & \text{if} \quad t < 0, \\ 1, & \text{if} \quad t \geq 0. \end{cases} \tag{4.29}$$

Furthermore, $T_i, \quad i = 1, \ldots, M$, are the durations needed for a 50% absorption of the insulin injected at time t_i, defined by

$$T_i = a_iD_i + b_i, \ i = 1, \ldots, M, \tag{4.30}$$

where D_i, measured in moles (M), is the insulin dose and a_i , b_i and s_i are specific to the type of insulin preparation administrated at time t_i. We assume that both the timing of each injection, t_i, and the corresponding dosage, $D_i, \ i = 1, \ldots, M$ are variables to be determined while the insulin type (i.e. the choice of each a_i, b_i and s_i) is specified by the user. Note that we have bounds on each dosage, i.e.

$$0 \leqslant D_i \leqslant D_{i,\max}, \ i = 1, \ldots, M. \tag{4.31}$$

4.3.2 Exercise modelling

It is well known that physical exercise has a significant effect on blood glucose levels. Indeed, one of the common ways to deal with mild cases of Type 2 diabetes is to prescribe increased exercise for patients along with sensible changes in diet. It is thus surprising to see that attempts to incorporate the effects of exercise into glucose-insulin dynamic models have only appeared in the literature relatively recently. This, together with the fact that most of the existing approaches have little to no overlap, seems to indicate that the task is not an easy one and that there are likely to be multiple pathways through which exercise impacts both glucose and insulin levels in the blood. In [16], the impact of exercise is modelled rather simply by perturbing coefficients in the well known Bergman minimal model [10]. The main aim in [16] is to study the stability properties of equilibria for different scenarios. Reference [11] follows a similar approach and also introduces some

additional dynamic states (energy consumption and insulin action). The main focus of [11] was to fit the resulting model to results from a clinical study. The authors of [22] start with a different glucose-insulin model [53] and emphasize the importance of the redistribution of blood flows around the body during periods of exercise. None of the models mentioned so far lend themselves to incorporation with the model described in Section 4.2, as they were all based on much simpler glucose-insulin models involving only 3 state variables. Reference [49] introduces a much more comprehensive model. This takes into account the important role of free fatty acids (FFAs) in the blood stream as a source of energy for the body. It is argued that there are important interactions between the levels of FFAs, insulin and exercise which have not been accounted for in previous models. While we are not incorporating the complete model from [49] into the one from Section 4.2 (this would be an interesting challenge for future studies), we are adopting several aspects related to the impact of exercise. First, it is argued that exercise promotes a clearance of insulin in the blood stream since this results in higher glucose production in the liver which is needed to provide energy. Mathematically, this is modelled as a second order effect with the dynamics

$$\frac{dx_9}{dt} = m_{pv}(u_{ex} - x_9), \tag{4.32}$$

$$\frac{dx_{10}}{dt} = m_{IU1}x_9 - m_{IU2}x_{10}, \tag{4.33}$$

where $x_9 \in [0, 100]$ represents the current percentage of the maximum rate of oxygen consumption for an individual (which, in turn, is assumed to be linearly proportional to the energy expenditure). Here, $u_{ex} \in [0, 100]$ is the rate of oxygen consumption due to exercise (itself measured as a percentage of the maximum rate of oxygen consumption for an individual) and x_{10} is the rate at which insulin is cleared from the blood due to this effect. Moreover, m_{pv} and m_{IU1} and m_{IU2} are model constants whose values are listed in Table 4.4. Thus, equation (4.27) is modified as follows

$$\frac{dx_2}{dt} = -(k^p_{2,1} + k^p_{2,2})x_2 + w_2 + \sum_{i=1}^{M} I_i - x_{10}x_2, \tag{4.34}$$

The authors of [49] also indicate that exercise induces an increase in the glucose uptake rate by the working muscles. Furthermore, the rate of glucose production is also increased due to an accelerated rate of glycogenolysis (conversion of glycogen into glucose-6-phospate which is further converted to glucose). These effects are modelled by the following dynamics,

$$\frac{dx_{11}}{dt} = m_{GU1}x_9 - m_{GU2}x_{11}, \tag{4.35}$$

Constant	Value	Unit
m_{pv}	0.8	min^{-1}
m_{IU1}	2.8176×10^{-3}	min^{-2}
m_{IU2}	1.7354	min^{-1}
m_{GU1}	2.1874×10^{-3}	$\text{mg}/(\text{kg}\times \text{min}^2)$
m_{GU2}	5.8974×10^{-2}	min^{-1}
m_{GP1}	9.152×10^{-4}	$\text{mg}/(\text{kg}\times \text{min}^2)$
m_{GP2}	1.3073	min^{-1}
W	32001.46	kg/l

Table 4.4: Parameter values related to exercise effect on glucose and insulin dynamics

$$\frac{dx_{12}}{dt} = m_{GP1}x_9 - m_{GP2}x_{12}, \tag{4.36}$$

where x_{11} and x_{12} represent the exercise induced glucose uptake and production rates, respectively. Furthermore, m_{GU1}, m_{GU2}, m_{GP1} and m_{GP2} are constants whose values are also listed in Table 4.4. Finally, the effects are incorporated into blood glucose dynamic equation (4.12) as follows.

$$\frac{dx_8}{dt} = -f_4 + f_5 - f_1 - f_2 f_3 + G + W(x_{12} - x_{11}), \tag{4.37}$$

where W is a model constant whose value is also given in Table 4.4.

4.3.3 Summary of the revised model

In summary, the dynamical model is described as follows. The dynamics for x_1 and x_2 are

$$\frac{dx_1}{dt} = -(k^p_{1,1} + k^p_{1,2})x_1 + w_1, \tag{4.38}$$

where w_1 is defined by equation (4.2), and

$$\frac{dx_2}{dt} = -(k^p_{2,1} + k^p_{2,2})x_2 + w_2 + \sum_{i=1}^{M} I_i - x_{10}x_2, \tag{4.39}$$

where w_2 and I_i are defined by equations (4.4) and (4.28), respectively.

The dynamics for x_3, x_4, x_5 and x_6 are

$$\frac{dx_3}{dt} = -k^s_{1,1}x_3(R^0_1 - x_5) - k^s_{1,2}x_3 + \frac{k^p_{1,1}V_p x_1}{V}, \tag{4.40}$$

$$\frac{dx_4}{dt} = -k^s_{2,1}x_4(R^0_2 - x_6) - k^s_{2,2}x_4 + \frac{k^p_{2,1}V_p x_2}{V}, \tag{4.41}$$

$$\frac{dx_5}{dt} = -k^s_{1,1}x_3(R^0_1 - x_5) - k^r_1 x_5, \tag{4.42}$$

$$\frac{dx_6}{dt} = -k^s_{2,1}x_4(R^0_2 - x_6) - k^r_2 x_6. \tag{4.43}$$

The dynamics for x_7 and x_8 are

$$\frac{dx_7}{dt} = f_4 - f_5, \tag{4.44}$$

$$\frac{dx_8}{dt} = -f_4 + f_5 - f_1 - f_2 f_3 + G + W(x_{12} - x_{11}), \tag{4.45}$$

where $f_1 - f_5$ and G are defined by equations (4.13), (4.14), (4.15), (4.10), (4.11) and (3.16), respectively.

The exercise subsystem which governs state variables x_9, x_{10}, x_{11} and x_{12} is

$$\frac{dx_9}{dt} = m_{pv}(u_{ex} - x_9), \tag{4.46}$$

$$\frac{dx_{10}}{dt} = m_{IU1}x_9 - m_{IU2}x_{10}, \tag{4.47}$$

$$\frac{dx_{11}}{dt} = m_{GU1}x_9 - m_{GU2}x_{11}, \tag{4.48}$$

$$\frac{dx_{12}}{dt} = m_{GP1}x_9 - m_{GP2}x_{12}. \tag{4.49}$$

The system (4.38)-(4.49) is subject to the following initial conditions.

$$x_1(0) = 1.4 \times 10^{-11}, \tag{4.50}$$
$$x_2(0) = 2 \times 6.945 \times 10^{-12}, \tag{4.51}$$
$$x_3(0) = 0, \tag{4.52}$$
$$x_4(0) = 0.01 \times 6.945 \times 10^{-12}, \tag{4.53}$$
$$x_5(0) = 0, \tag{4.54}$$
$$x_6(0) = 0, \tag{4.55}$$
$$x_7(0) = 200, \tag{4.56}$$
$$x_8(0) = 918, \tag{4.57}$$
$$x_9(0) = 0, \tag{4.58}$$
$$x_{10}(0) = 0, \tag{4.59}$$
$$x_{11}(0) = 0, \tag{4.60}$$
$$x_{12}(0) = 0. \tag{4.61}$$

The complete composite model defined by equations (4.38)-(4.61) includes the model constants listed in Tables 4.2, 4.3 and 4.4. We again assume that the system is modelled over a 9 hour period, i.e., $t \in [0, 540]$, where t is the time in minutes.

4.4 Optimal control

4.4.1 Problem statement

We first formulate a combined optimal control and optimal parameter selection problem based on the composite model (4.38)-(4.61) for a diabetic individual. Our aim is to match the subject's blood glucose level with a desired blood glucose profile $g_d(t)$ over the entire time horizon. Thus, we need to choose injection times $t_i, i = 1, \ldots, M$, injection dosages $D_i, i = 1, \ldots, M$, and an exercise regime $u_{ex}(t)$, $t \in [0, 540]$, with the aim to minimize

$$J = \int_0^{540} \left(x_8(t) - g_d(t)\right)^2 dt \tag{4.62}$$

subject to the dynamics (4.38)-(4.61), subject to the control bounds

$$0 \leqslant u_{ex}(t) \leqslant 100, \tag{4.63}$$

and subject to

$$0 \leqslant t_i \leqslant 540, \ i = 1, \ldots, M \tag{4.64}$$

as well as the bounds on the dosages equation (4.31).

4.4.2 Control parameterization

For computational purposes, we assume that $u_{ex}(t)$ is a piecewise constant function defined over a partition $P = \{\tau_0, \tau_1, \ldots, \tau_N\}$ with $\tau_0 = 0$, $\tau_N = 540$ and $\tau_{i-1} \leqslant \tau_i, i = 1, \ldots, N$, where N is the number of intervals in the partition chosen by the user. Thus, $u_{ex}(t)$ may be written as

$$u_{ex}(t) = \sum_{i=1}^{N} \sigma_i \chi_{[\tau_{i-1}, \tau_i)}(t), \tag{4.65}$$

where σ_i is the chosen value of u_{ex} in the i-th interval, with

$$0 \leqslant \sigma_i \leqslant 100, \quad i = 1, \ldots, N, \tag{4.66}$$

and

$$\chi_{[\tau_{i-1}, \tau_i)}(t) = \begin{cases} 1, & \text{if} \quad t \in [\tau_{i-1}, \tau_i), \\ 0, & \text{otherwise.} \end{cases} \tag{4.67}$$

For convenience, note that we also assume that the insulin injection times $t_i, i = 1, \ldots, M$, coincide with some of the switching times of u_{ex}, i.e.

$$t_i = \tau_{k_i}, \ i = 1, \ldots, M, \tag{4.68}$$

where $k_i \in K = \{k_1, k_2, \ldots, k_M\} \subset \{\tau_0, \tau_1, \ldots, \tau_N\}$. Naturally, we also assume that $N >> M$.

4.4.3 Time scaling transformation

As noted above, MISER3.3 is not equipped to handle the variable time points $\tau_i, i = 1, \ldots, N$. Thus, we invoke a well known transformation [30] to map these variable time points to fixed points in a new time horizon $[0, N]$. This is achieved by defining a new time variable $s \in [0, N]$ and setting

$$\frac{dt(s)}{ds} = v(s), \tag{4.69}$$

where

$$v(s) = \sum_{i=1}^{N} \theta_i \chi_{[i-1, i]}(s), \tag{4.70}$$

and $\theta_i = \tau_i - \tau_{i-1},\ i = 1, \ldots, N$. Furthermore, we require

$$t(0) = \tau_0 = 0 \tag{4.71}$$

and

$$t(N) = T = 540. \tag{4.72}$$

Note that $\theta_i, i = 1, \ldots, N$, are now decision variables in the transformed problem and the values of $\tau_i, i = 1, \ldots, N$, can be easily calculated from $\theta_i,\ i = 1, \ldots, N$. Furthermore, we require

$$0 \leqslant \theta_i \leqslant T = 540, \quad i = 1, \ldots, N, \tag{4.73}$$

We adopt the notation $\tilde{x}_i(s) = x_i(t(s)), i = 1, \ldots, 12$, $\tilde{g}_d(s) = g_d(t(s))$ and $\tilde{u}_{ex}(s) = u_{ex}(t(s))$. Under the time scaling transformation, the dynamic system can be described as follows. The dynamics for x_1 and x_2 become

$$\frac{d\tilde{x}_1}{ds} = (-(k^p_{1,1} + k^p_{1,2})\tilde{x}_1 + w_1)v, \tag{4.74}$$

$$\frac{d\tilde{x}_2}{ds} = (-(k^p_{2,1} + k^p_{2,2})\tilde{x}_2 + w_2 + \sum_{i=1}^{M} \tilde{I}_i - \tilde{x}_{10}\tilde{x}_2)v, \tag{4.75}$$

where w_1, w_2 are as defined previously in equations (4.2) and (4.4), respectively. Moreover, $\tilde{I}_i(s) = I_i(t(s)), i = 1, \ldots, M$, The dynamics for x_3, x_4, x_5 and x_6 become

$$\frac{d\tilde{x}_3}{ds} = (-k^s_{1,1}\tilde{x}_3(R^0_1 - \tilde{x}_5) - k^s_{1,2}\tilde{x}_3 + \frac{k^p_{1,1}V_p\tilde{x}_1}{V})v, \tag{4.76}$$

$$\frac{d\tilde{x}_4}{ds} = (-k^s_{2,1}\tilde{x}_4(R^0_2 - \tilde{x}_6) - k^s_{2,2}\tilde{x}_4 + \frac{k^p_{2,1}V_p\tilde{x}_2}{V})v, \tag{4.77}$$

$$\frac{d\tilde{x}_5}{ds} = (-k^s_{1,1}\tilde{x}_3(R^0_1 - \tilde{x}_5) - k^r_1\tilde{x}_5)v, \tag{4.78}$$

$$\frac{d\tilde{x}_6}{ds} = (-k^s_{2,1}\tilde{x}_4(R^0_2 - \tilde{x}_6) - k^r_2\tilde{x}_6)v. \tag{4.79}$$

The dynamics for x_7 and x_8 become

$$\frac{d\tilde{x}_7}{ds} = (f_4 - f_5)v, \tag{4.80}$$

$$\frac{d\tilde{x}_8}{ds} = (-f_4 + f_5 - f_1 - f_2f_3 + \tilde{G} + W(\tilde{x}_{12} - \tilde{x}_{11}))v, \tag{4.81}$$

where $f_1, \ldots, f_5$ are defined by (4.13), (4.14), (4.15), (4.10) and (4.11), respectively, and $\tilde{G}(s) = G(t(s))$.

The exercise subsystem dynamics become

$$\frac{d\tilde{x}_9}{ds} = m_{pv}(\tilde{u}_{ex} - \tilde{x}_9)v, \tag{4.82}$$

$$\frac{d\tilde{x}_{10}}{ds} = (m_{IU1}\tilde{x}_9 - m_{IU2}\tilde{x}_{10})v, \tag{4.83}$$

$$\frac{d\tilde{x}_{11}}{ds} = (m_{GU1}\tilde{x}_9 - m_{GU2}\tilde{x}_{11})v, \tag{4.84}$$

$$\frac{d\tilde{x}_{12}}{ds} = (m_{GP1}\tilde{x}_9 - m_{GP2}\tilde{x}_{12})v. \tag{4.85}$$

The dynamics of the new state variable $t(s)$ is

$$\frac{dt(s)}{ds} = v(s), \tag{4.86}$$

where v is defined by equation (4.70).
The transformed problem may now be stated as: Choose $v(s), \tilde{u}_{ex}(s), t_i$ and $D_i, i = 1, \ldots, M$, so as to minimize

$$\tilde{J} = \int_0^N v(s)\left(\tilde{x}_8(s) - \tilde{g}_d(s)\right)^2 ds \tag{4.87}$$

subject to the dynamics (4.74)-(4.86), the initial conditions (4.50) to (4.61) with $t(0) = 0$, the parameter bounds: (4.31), (4.66) and (4.73), and subject to the constraints

$$g_i = t(k_i) - t_i = 0, i = 1, \ldots, M, \tag{4.88}$$

$$g_{n+1} = T - t(N) = 0. \tag{4.89}$$

There is one feature in the transformed problem which prevents its direct implementation in MISER3.3. In the transformed objective (4.87), we have the function $g_d(t(s))$, where $t(s)$ is a state variable in the transformed problem. Recall from Chapter 1 that MISER3.3 assumes differentiability of the objective integrand with respect to the state variables. However, when choosing $g_d(t(s)) = g_{exp}(t(s))$ as defined in Section 4.2.4, this piecewise linear function is not differentiable with respect to t. Thus, we change the g_{exp} from a linear form to a quadratic form defined in equation (4.90) below and illustrated in Figure 4.2:

$$\tilde{g}_d = \alpha_i t(s)^2 + \beta_i t(s) + \gamma_i, \quad t(s) \in [t_{i-1}(s), t_i(s)], \ i = 1, \ldots, 8, \tag{4.90}$$

i	α_i	β_i	γ_i
1	$-1.182857143 \times 10^{-3}$	0.1656	5
2	-9.178×10^{-4}	0.128492	6.29878
3	$1.828555556 \times 10^{-3}$	-0.5306333333	45.8463
4	-7.85×10^{-4}	0.2534333333	-12.9587
5	$4.003055556 \times 10^{-4}$	-0.1732766667	25.4452
6	$-1.720357143 \times 10^{-4}$	0.1014471429	-7.521657143
7	6.098125×10^{-4}	-0.4927575	105.3772250
8	$-2.308472222 \times 10^{-4}$	0.2133966667	-42.91515

Table 4.5: Parameter values of the g_d function as quadratic form

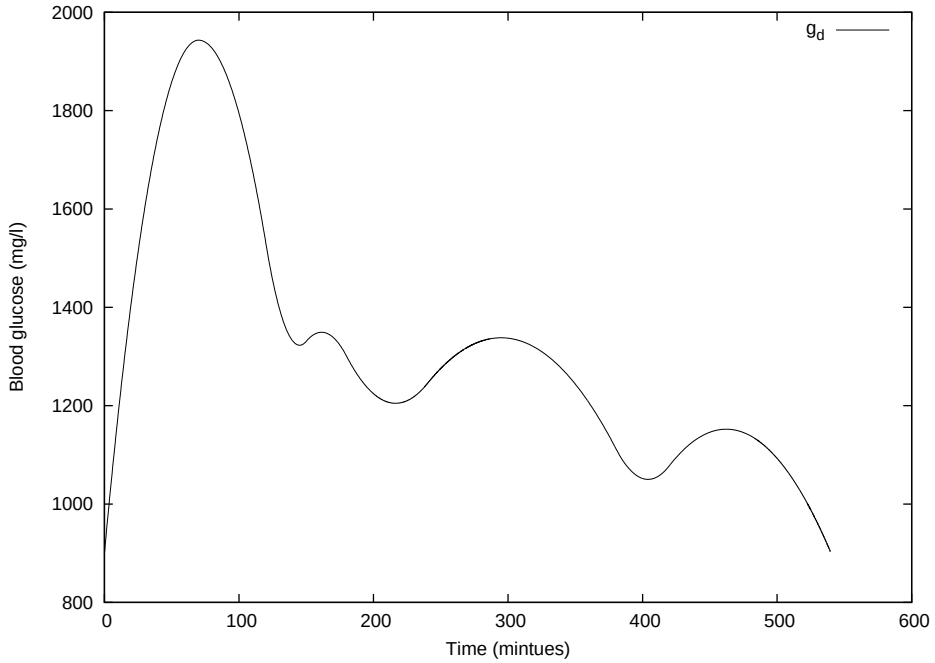

Figure 4.2: Experimental data in quadratic form

The parameter values defining this function are determined from a smooth piecewise quadratic interpolation of the data in Table 4.1 and they are listed in Table 4.5. In summary, the transformed dynamic model consists of 13 state variables, $\tilde{x}_i(s), i = 1, \ldots, 12$ and $t(s)$, 2 control functions, $\tilde{u}_{ex}(s)$ and $v(s)$, and $2M$ system parameters, $D_i, i = 1, \ldots, M$, and $t_i, i = 1, \ldots, M$. These system parameters represent, respectively, the volume of insulin injections and time points of these injections. In this model, the orig-

inal time $t \in [0, 540]$ is transformed to a new time scale $s \in [0, N]$. For the numerical results presented below, we assume up to $M = 5$ individual injections. We also assume $N = 20$ and choose $k_1 = 0$, $k_2 = 4$, $k_3 = 8$, $k_4 = 12$ and $k_5 = 16$ for the constraints given in (4.88). Finally, the bounds on the control functions (equivalent to the parameter bounds (4.66) and (4.73)) are

$$0 \leqslant \tilde{u}_{ex}(s) \leqslant 100, \quad \text{and} \quad 0 \leqslant v(s) \leqslant 540, \quad s \in [0, 20]. \tag{4.91}$$

This version of the problem is in a a canonical form suitable for MISER3.3.

4.5 Numerical results

4.5.1 Case 1

The first case that we tested is for a type 1 diabetic (R_m=0) with only one intermediate acting insulin (NPH) injection at the beginning of the time horizon ($t_1 = 0$) and with no exercise. Here, we assume that the desired blood glucose function is $g_d(t) = g_{exp}(t)$, where g_{exp} is in quadratic form as shown in Figure 4.2. This means that we are effectively trying to emulate the blood glucose level of a healthy individual. This is a relatively simple version of the problem with only one decision variable (D_1), the dosage of insulin injected at $t_1 = 0$, where

$$0 \leqslant D_1 \leqslant 2.778 \times 10^{-04}. \tag{4.92}$$

An optimal solution is readily obtained by MISER3.3. Figure 4.3 shows that the optimal blood glucose trajectory follows the desired blood glucose profile only briefly near the beginning of the time horizon. The optimal value of insulin injection D_1 is $2.28728 \times 10^{-04}M$ which is equivalent to $32U$. Clearly, one injection is not enough to achieve a good glucose control over the entire time horizon and we will need to consider multiple injections as well as exercise.

4.5.2 Case 2: Transformed composite model with exercise

This case also assumes a type 1 diabetic ($R_m = 0$) and we once again use $g_d(t) = g_{exp}(t)$. We consider two different types of insulin preparations, intermediate and short acting in combination. Details of the bounds and initial guesses of t_i, $i = 1, \ldots, 5$, are given in Table 4.6. The bounds on the dosages are given in equation (4.93). Note that either intermediate or slow acting insulin may be chosen for each injection and corresponding values of a_i, b_i and $s_i, i = 1, \ldots, M$, must also be chosen. We indicate the values in table 4.7. In this case, we assume that the first injection is an intermediate acting insulin while

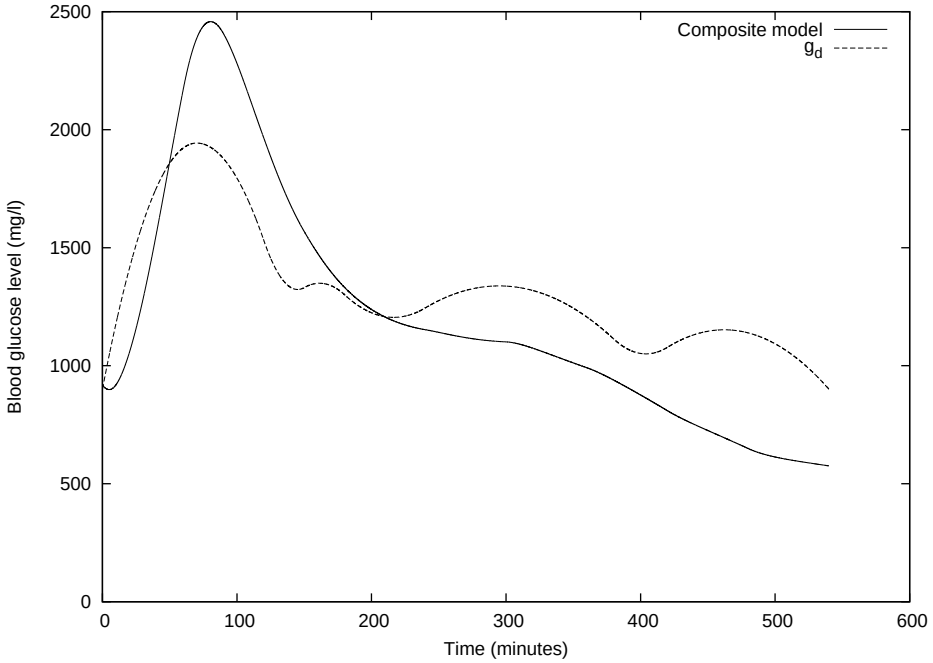

Figure 4.3: Comparison of two blood glucose trajectories: the solid curve is the optimal trajectory for Case 1. The dashed curve is the desired trajectory

subsequent injections alternate between short and intermediate acting.

$$0 \leqslant D_i \leqslant 2.0835 \times 10^{-04}, \quad i = 1, \ldots, 5. \tag{4.93}$$

A combination of different types of insulin injections as well as exercise yields better results as shown in Figure 4.4. Figure 4.5 shows the optimal exercise level and Table 4.8 shows the optimal values of decision variables D_i and t_i, $i = 1, \ldots, 5$. Note that effectively just one injection is administered while exercise is used for most of the time horizon.

Decision variables t_i	**Initial guess**	**Lower bound**	**Upper bound**
t_1	0	0	540
t_2	108	0	540
t_3	216	0	540
t_4	324	0	540
t_5	432	0	540

Table 4.6: Decision variable t_i

Insulin dosage D_i	Parameter values		
	s_i	a_i	b_i
D_1	2	1.5550756×10^6	294
D_2	2	4.31965×10^5	102
D_3	2	1.5550756×10^6	294
D_4	2	4.31965×10^5	102
D_5	2	1.5550756×10^6	294

Table 4.7: Insulin dosages and their corresponding parameter values of a_i, b_i and $s_i, i = 1, \ldots, 5$.

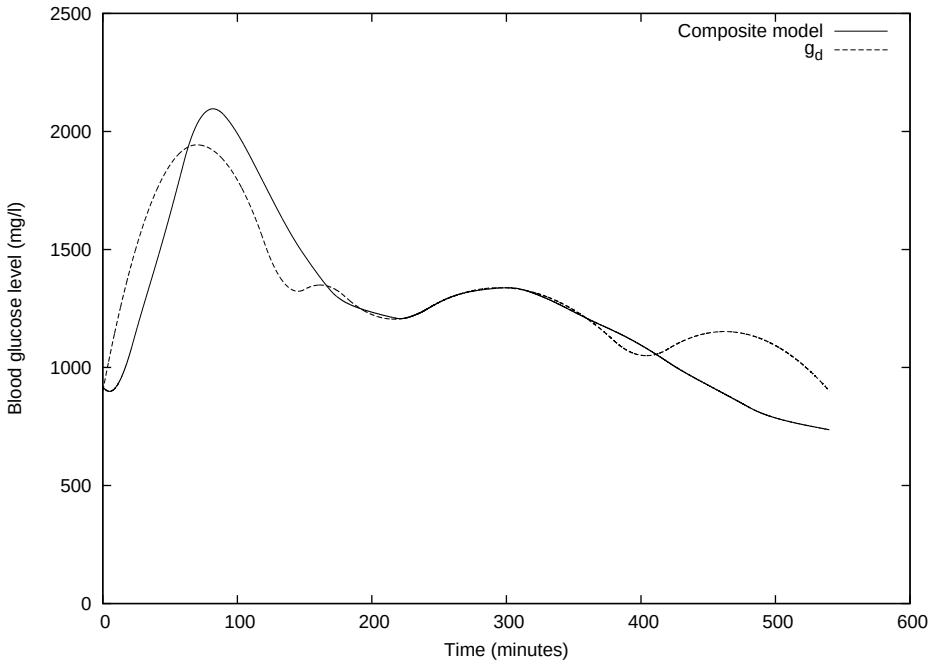

Figure 4.4: Blood glucose trajectories for Case 2.

4.5.3 Case 3: Composite model without exercise

All details for this case are the same as those for Case 2, except that we assume no exercise here, i.e. $u_{ex}(t) = 0, t \in [0, 540]$.

As shown in Figure 4.6, the resulting blood glucose level still tracks the desired blood glucose profile reasonably well. Note that the optimal solution involves a combination of 2 insulin types.

4.5.4 Case 4: Composite model for type 2 diabetes

In order to test the composite model for a type 2 diabetic case, we halve the original insulin feedback rate ($R_m = 0.5$). Here exercise is once again considered and the same

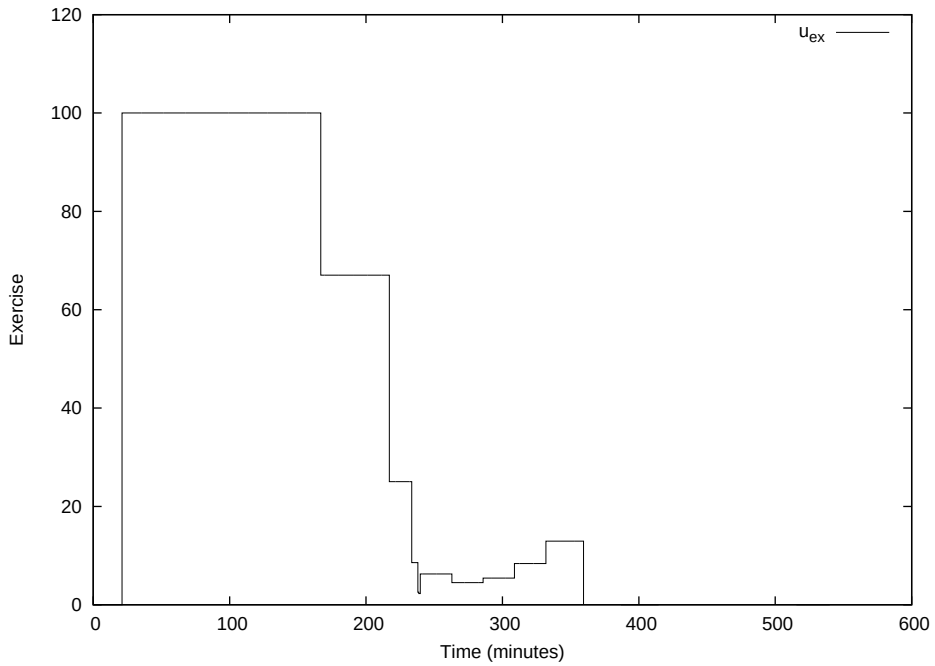

Figure 4.5: Optimal exercise level for Case 2.

types of insulin combinations as used in Cases 2 and 3 are assumed.

Clearly, Figure 4.7 shows that the resulting blood glucose level tracks the desired blood glucose profile very closely. Figure 4.8 shows the corresponding optimal exercise level. Also, the optimal values of insulin injections are listed in Table 4.10. Note that a much lower dosage of insulin along with an earlier use of exercise is sufficient to manage good blood glucose control in this case.

Insulin injections D_i	**Optimal values**	**Injection times** t_i	**Optimal values**
D_1	$1.70822 \times 10^{-04} M \equiv 24U$	t_1	0
D_2	0	t_2	217.06
D_3	0	t_3	239.789
D_4	0	t_4	331.894
D_5	0	t_5	441.96

Table 4.8: Optimal values of decision variables D_i and t_i in Case 2

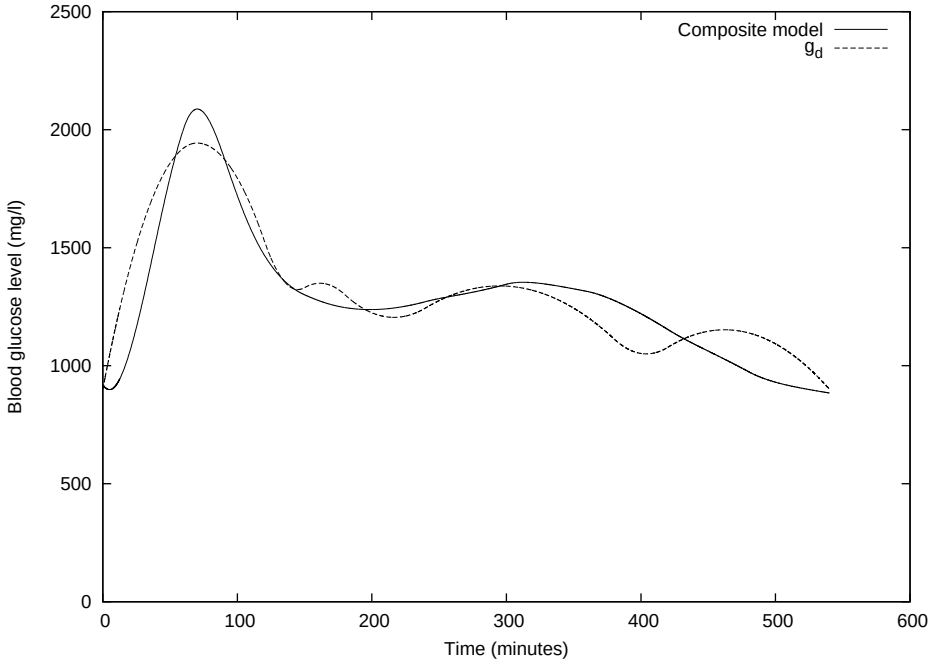

Figure 4.6: Blood glucose levels resulting from optimization of the model without exercise for Case 3

4.5.5 Case 5: Aiming for basal blood glucose level

In this case, we once again consider a type 1 diabetic ($R_m = 0$) and we adopt the objective function

$$\tilde{J} = \int_0^N v(s)\left(\tilde{x}_8(s) - 918\right)^2 ds \tag{4.94}$$

which simply penalizes any blood glucose deviation from the initial level. The problem is to minimize (4.94) subject to the same dynamic model (4.38)-(4.61) as in previous cases.

Insulin injections D_i	**Optimal values**	**Injection times** t_i	**Optimal values**
D_1	$1.16789 \times 10^{-04} M \equiv 16U$	t_1	0
D_2	$5.08087 \times 10^{-05} M \equiv 7.3U$	t_2	12.6863
D_3	0	t_3	203.28
D_4	0	t_4	327.639
D_5	0	t_5	439.112

Table 4.9: Optimal values of decision variables D_i and t_i in Case 3

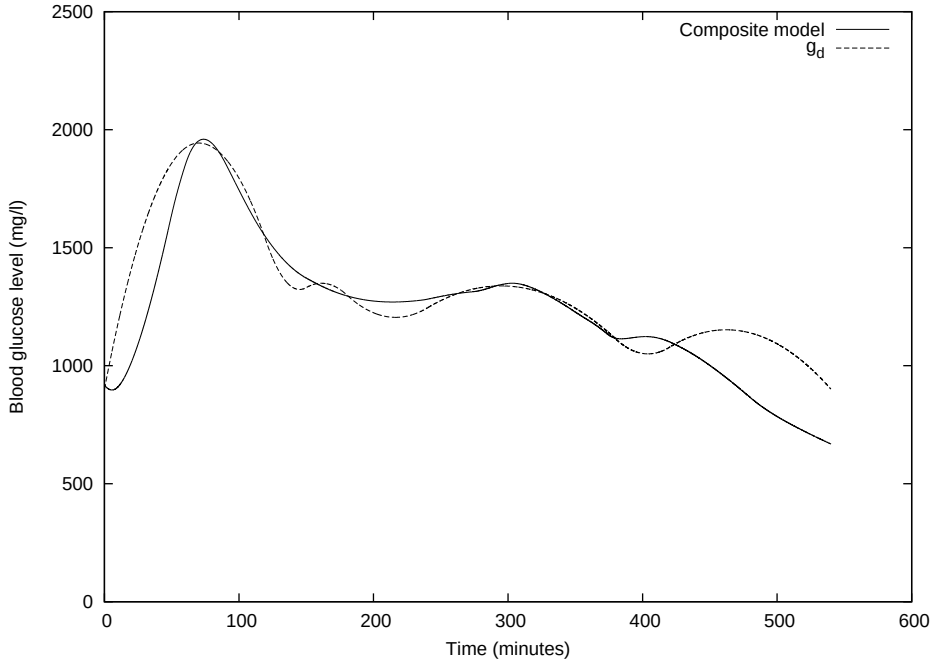

Figure 4.7: Blood glucose levels resulting for Case 4.

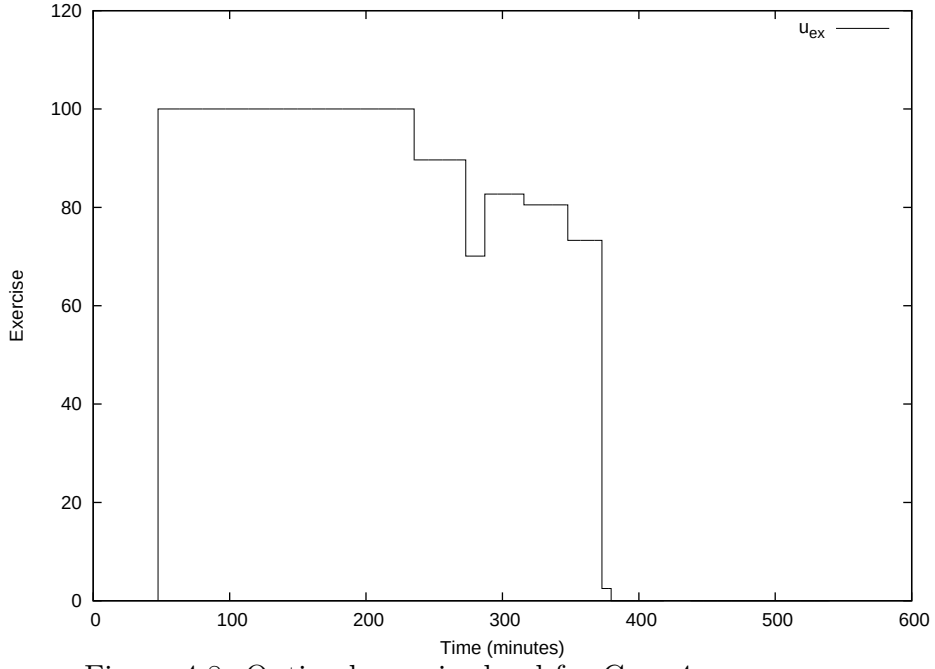

Figure 4.8: Optimal exercise level for Case 4.

All details for this case are the same as those of Case 2, except for the objective function and the assumed order of the insulin injections. We again assume that insulin injections

Insulin injections D_i	**Optimal values**	**Injection times** t_i	**Optimal values**
D_1	0	t_1	0
D_2	$1.77675 \times 10^{-5} M \equiv 2.5U$	t_2	47.4842
D_3	0	t_3	273.071
D_4	0	t_4	372.92
D_5	0	t_5	437.78

Table 4.10: Optimal values of decision variables D_i and t_i in Case 4

have an alternating pattern, but this time starting with a short acting insulin.

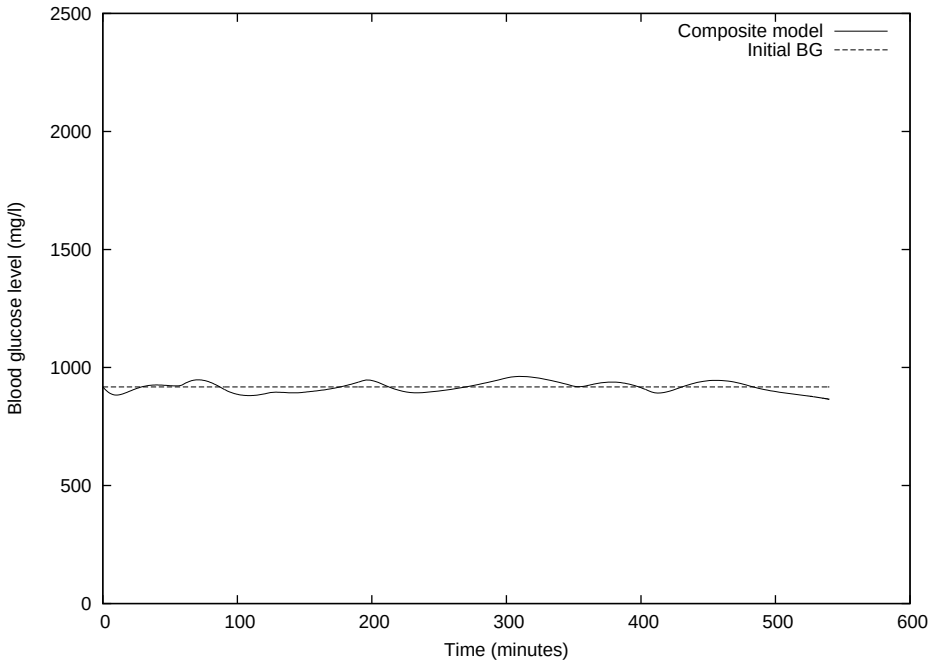

Figure 4.9: Blood glucose levels resulting from Case 5.

As can be seen from Figure 4.9, the optimal blood glucose level resulting in this case remains very close to the initial blood glucose level (918 mg/l= 5.1 mmol/l) over the entire time horizon. Figure 4.10 shows the optimal exercise level and Table 4.11 shows the optimal values of the decision variables D_i and $t_i, i = 1, \ldots, 5$. Due to the need to clear a lot of glucose early on, multiple insulin injections early in the time horizon combined with an early high level of exercise are required in this case.

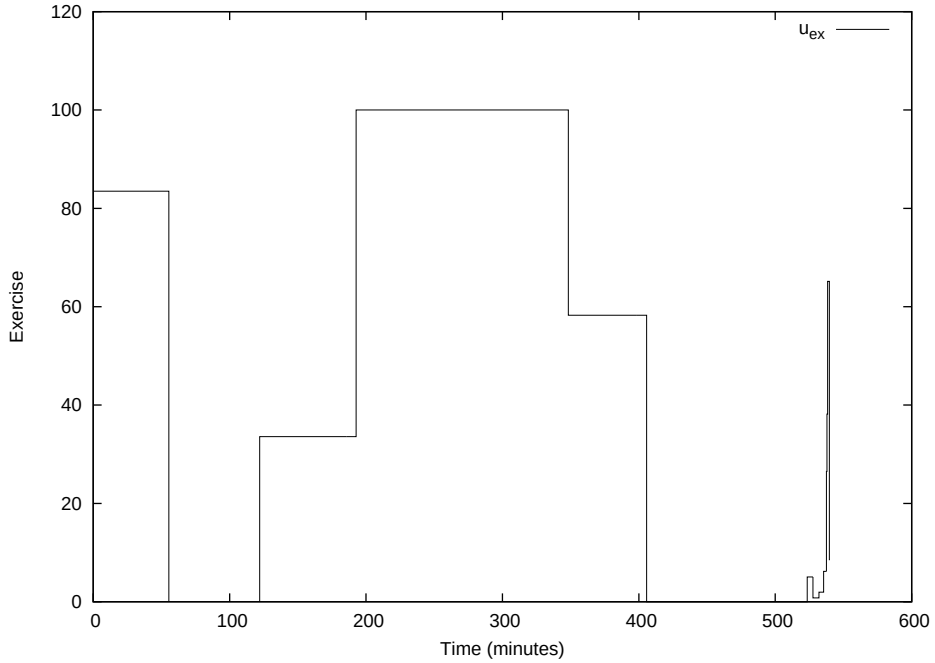

Figure 4.10: Optimal exercise level in Case 5.

4.6 Conclusions

We have developed a composite model that is capable of capturing the effects of exercise and subcutaneous insulin injections. This model is based on the dynamical model of the blood glucose regulatory system presented in [3]. Levels of exercise are described in terms of the percentage of the maximum rate of oxygen consumption for an individual and exercise is assumed to lead to higher levels of energy consumption and lower levels of blood insulin. The appearance of blood insulin as a result of subcutaneous injections is modelled according to a robust model proposed by Berger et al. [8].

Insulin injections D_i	**Optimal values**	**Injection times t_i**	**Optimal values**
D_1	$1.31322 \times 10^{-04} M \equiv 18U$	t_1	0
D_2	$6.27708 \times 10^{-05} M \equiv 9U$	t_2	121.984
D_3	0	t_3	523.462
D_4	0	t_4	523.462
D_5	0	t_5	537.528

Table 4.11: Optimal values of decision variables D_i and t_i in Case 5

Based on this new dynamic model, we then formulate a combined optimal control and optimal parameter selection problem with the objective of matching a desired blood glucose profile as closely as possible. This problem involves variable switching times for the control as well as multiple variable characteristic times in the dynamics. To make this problem suitable for the optimal control software MISER3.3, a time scaling transformation was invoked. We formulated a variety of cases to test the model. These included type 1 or 2 diabetic subjects, a single insulin injection at $t = 0$, multiple insulin injections with or without exercise and two distinct desired blood glucose profiles. While a single insulin injection alone did not result in good blood glucose control, all other cases resulted in effective control.

This work represents the first application of a range of recent advances in the area of computational optimal control to diabetes models and there is significant scope for future work in this regard. For example, just as we allowed for multiple insulin injection times, it should be possible to incorporate multiple meals and also optimize the timing of these meals. Another interesting challenge would be the incorporation of free fatty acids (FFAs) into the model [49], since these also represent an important energy source for the body. One should also investigate the possibility of incorporating other types of treatments typical for type 2 diabetics.

CHAPTER 5

Conclusions

5.1 Main contributions of this thesis

This thesis has been concerned with the disease of diabetes, one of the major global health problems threatening the wellbeing of humanity worldwide. A permanent cure for this disease has been elusive until now, but it can be managed. This thesis proposes and illustrates a general methodology for the analysis and control of the human blood glucose regulatory system. In addition, it demonstrates that computational optimal control methods can be readily used to determine open loop optimal controls for dynamic models of the blood glucose regulatory system, particularly in the context of diabetes. While open loop controls do not take into account modelling errors and uncertainties in systems, they still provide a useful benchmark for the performance of other more practical control strategies. Using this approach, we can also test extreme scenarios on models and thus identify their weaknesses.

In Chapter 1, the first section is devoted to a brief discussion about diabetes; its diagnosis, causes and consequent health problems that can result in the long term. It describes the natural cycle of regulating the blood glucose level in the human body, which is directed by the regulator hormones insulin and glucagon. It also describes in detail a variety of factors that impact the blood glucose level in the human body. Then various management strategies for diabetes are reviewed. From a mathematical point of view, control methods of diabetes generally rely on dynamical models of the body's blood glucose regulatory system. The remaining sections of Chapter 1 describe the basic concepts of optimal control theory. This includes general formulations of optimal control and optimal parameter selection problems, followed by a brief description of two solution techniques used in the thesis, control parameterization and a time scaling transformation. The powerful optimal control software MISER3.3 [25] is used throughout the thesis to produce computational numerical results for a variety of scenarios related to this problem.

Chapter 2 gives a detailed review of mathematical models for the human blood glucose regulatory system. This includes a range of algorithms to control blood glucose in diabet-

ics. For each of these, their main features and respective contributions to the field have been outlined. However, very few of these algorithms are based directly on underlying nonlinear models and thus they cannot take full advantage of the assumed nonlinearities. The only work reviewed in Chapter 2 that uses computational optimal control methods on the basis of a nonlinear model is [14]. Since its publication, significant advances have been made in the area of computational optimal control. In particular, we are now able to deal with problems with variable decision points in the time horizon and these time points may also appear in the objective function and in the dynamics.

The main original contributions of this thesis are given in Chapters 3 and 4, where we refine, extend, test and optimize an existing model of intermediate complexity.

In Chapter 3, we adopt a comprehensive model of the blood glucose regulatory system from Liu and Tang [31]. Based on their dynamic model, we formulate an optimal parameter selection problem. The purpose of this formulation is to obtain more reasonable values for many of the model parameters in the Liu and Tang model whose values are difficult to determine directly. The objective in this formulation is to fit the blood glucose trajectory resulting from the model as closely as possible to real data [27]. Existing approaches generally just involve educated guesses of the values for these model constants. Furthermore, these constants can vary significantly between different subjects, and even over time for the same subject, so there is clearly a need for simple and robust methods to determine values for them. We investigated several different model matching objectives and found that significant improvements in matching the model to desired data was achieved in all cases compared to the original results in Liu and Tang [31]. It is hard to judge the relative quality of these results and the ultimate choice is best left to experts who are more familiar with the use of the model in relation to the real physical system. Nevertheless, we have demonstrated that the proposed model matching strategy yields very good results in this scenario. There is a wide variety of other biological systems for which the same methodology should also prove useful (see for example [4], [6] and [42]). We also found that the optimized model was more sensitive to changes in the insulin release rate (R_m) proposed by Liu and Tang, but this is to be expected. Furthermore, we formulated an open loop optimal control problem to determine optimal rates of insulin and glucagon secretion and showed how it can be readily solved by MISER3.3. In contrast, the authors in [31] considered this problem too difficult to solve.

In Chapter 4, we have developed a composite model that is also capable of capturing the effects of exercise and subcutaneous insulin injections, based on the dynamical model of the blood glucose regulatory system studied in Chapter 3. Levels of exercise are described in terms of the percentage of the maximum rate of oxygen consumption for an individual and exercise is assumed to lead to higher levels of energy consumption and lower levels of blood insulin. The appearance of blood insulin as a result of subcutaneous

injections is modelled according to a robust model proposed by Berger et al. [8].

Based on this new dynamic model, we then formulated a combined optimal control and optimal parameter selection problem with the objective of matching a desired blood glucose profile as closely as possible. This problem involves variable switching times for the control as well as multiple variable characteristic times in the dynamics. To make this problem suitable for the optimal control software MISER3.3, a time scaling transformation was invoked. We formulated a variety of cases to test the model. These included type 1 or type 2 diabetic subjects, a single insulin injection at $t = 0$, multiple insulin injections with or without exercise and two distinct desired blood glucose profiles. While a single insulin injection alone did not result in good blood glucose control, all other cases resulted in effective control. Thus, we have demonstrated that good blood glucose can be achieved given moderate levels of treatment. The new model is a more integrated and comprehensive model for the regulation of blood glucose levels in diabetics compared to many existing models.

In summary, the work in Chapter 4 represents the first application of a range of recent advances in the area of computational optimal control to diabetes models and there are many ways to extend both the model and the solution algorithms as detailed below.

5.2 Future research directions

We have reviewed a variety of mathematical models of the blood glucose regulatory system and associated control algorithms for diabetics. A new methodology for matching such models to actual data has been proposed and demonstrated to work well. Finally, we have presented a new mathematical model by extending the Liu and Tang model [31] in two ways. We discuss some additional possible improvements to the new composite model below.

(i) In the Liu and Tang approach [31], to test the validity and credibility of their model, they checked how the model fits experimental data reported in Korach-André et al. [27]. We used the same experimental data in all our numerical results. This data set consists of blood glucose measurements from a healthy individual taken after meals. Future studies should perhaps consider different data sources or use combined data from a larger sample set. It would also be interesting to test how well the model fit continues to match an individual over time.

(ii) In Chapter 4, just as we allow the new composite model to include multiple injection times, it should be possible to incorporate multiple meal times (glucose sources) into the model instead of only one meal. We may then also optimize the timing of these

as another obvious treatment strategy. More accurate submodels of the digestive tract may be needed in this case [37].

(iii) An interesting challenge would be the incorporation of free fatty acids (FFAs) into the model, since these also represent an important energy source for the body. Roy and Parker in [49] proposed a comprehensive model that takes into account the important role of FFAs in the blood stream as a source of energy for the body. Its dynamics consider important interactions between the levels of FFAs with exercise, FFAs with glucose and FFAs with insulin concentration.

(iv) Finally, there are a variety of common medical treatments used for type 2 diabetics before the need for insulin injections. Clearly, it would be of great benefit to allow for these treatments in our dynamic blood glucose regulatory model and consider combined treatment regimes with a much wider variety of options. However, as noted below, it is not always clear how these treatments can be adopted in the current model or what extensions to the model are needed in order to do so. Progress here will likely require input from practitioners more familiar with the underlying biological processes. We consider a variety of the most common non-insulin treatment options below.

For ease of reference, we recall the Liu and Tang model from Chapter 2 at this point.

$$\frac{dx_1}{dt} = -(k^p_{1,1} + k^p_{1,2})x_1 + w_1, \tag{5.1}$$

where

$$w_1 = \frac{G_m}{1 + b_1 \exp a_1(x_8 - C_5)}, \tag{5.2}$$

$$\frac{dx_2}{dt} = -(k^p_{2,1} + k^p_{2,2})x_2 + w_2, \tag{5.3}$$

and

$$w_2 = \frac{R_m}{1 + b_2 \exp a_2(C_1 - x_8)}. \tag{5.4}$$

$$\frac{dx_3}{dt} = -k^s_{1,1}x_3(R^0_1 - x_5) - k^s_{1,2}x_3 + \frac{k^p_{1,1}V_p x_1}{V}, \tag{5.5}$$

$$\frac{dx_4}{dt} = -k^s_{2,1}x_4(R^0_2 - x_6) - k^s_{2,2}x_4 + \frac{k^p_{2,1}V_p x_2}{V}, \tag{5.6}$$

$$\frac{dx_5}{dt} = -k^s_{1,1}x_3(R^0_1 - x_5) - k^r_1 x_5, \tag{5.7}$$

$$\frac{dx_6}{dt} = -k^s_{2,1}x_4(R^0_2 - x_6) - k^r_2 x_6. \tag{5.8}$$

$$\frac{dx_7}{dt} = f_4 - f_5, \tag{5.9}$$

where

$$f_4 = \frac{k_1 x_6}{1 + k_2 x_5} \cdot \frac{V_{\max}^{gs} x_8}{k_m^{gs} + x_8}, \tag{5.10}$$

$$f_5 = k_3 x_5 \frac{V_{\max}^{gp} x_7}{k_m^{gp} + x_7}, \tag{5.11}$$

and

$$\frac{dx_8}{dt} = -f_4 + f_5 - f_1 - f_2 f_3 + G, \tag{5.12}$$

where

$$f_1 = U_b \left(1 - \exp\left(-\frac{x_8}{C_2}\right)\right), \tag{5.13}$$

$$f_2 = \frac{x_8}{C_3}, \tag{5.14}$$

$$f_3 = U_0 + \frac{(U_m - U_0) x_4^{\beta}}{C_4^{\beta} + x_4^{\beta}}. \tag{5.15}$$

(1) Metformin is usually the first medication prescribed for type 2 diabetic patients. It has a long history of usage in humans and was introduced in some countries as early as the 1960s. Although some users experience gastrointestinal irritation as a side effect, metformin is widely used and is considered to be very effective in the early stages of type 2 diabetes. While the molecular mechanism of metformin is not completely understood, its primary effect is to significantly reduce hepatic gluconeogenesis (production of glucose in the liver). This is normally elevated in type 2 diabetic patients. Additional effects of metformin include the increased insulin sensitity of cells (leading to increased uptake of glucose) and a decreased absorption of glucose from the digestive system [7].

While reduced hepatic gluconeogenesis and increased insulin sensitivity may be incorporated into our model by changing the model constants in equations (5.11) and (5.13)- (5.15), respectively, the latter effect will likely require a more complete dynamic model that includes the details of the digestive processes.

(2) Gliclazide is another common oral medication for type 2 diabetics. It essentially stimulates the pancreas to release more insulin and works by binding itself to certain receptors on the surface of pancreatic beta cells. Side effects of taking gliclazide are rare, but patients must be careful not to over dose on this medication as it can quickly lead to hypoglycemia [45]. Given its action, it

should be possible to incorporate the effects of gliclazide by modifying one or more of the constants in the insulin release rate in equation (5.4).

(3) Exenatide (sold under the trade names Byetta and Bydureon) is a more recently introduced treatment option that is often prescribed when metformin is no longer sufficient to control the effects of type 2 diabetes. Unlike the oral medications above, exenatide has to be injected subcutaneously. There is a higher chance of side effects with the use of exenatide, particularly gastrointestinal irritation. However, in the absence of side effects, exenatide has several benefits for type 2 diabetics. It stimulates the pancreas to release more insulin in response to consuming carbohydrates, it reduces the amount of glucagon released from the pancreas after a meal (which in turn reduces hepatic gluconeogenesis), it slows down the passage of food from the stomach to the gut and consequently gives an increased feeling of fullness. The latter effects are probably responsible for the weight loss that is widely observed for patients who take exenatide. The mechanisms by which exenatide achieves these effects are not well understood and it is consequently more difficult to incorporate these into our existing model.

(4) A range of other medicines are also available for the treatment of type 2 diabetes. They work in manners similar to those mentioned above and thus their possible incorporation into our existing model also follows along the lines mentioned in points 1-3. Amongst the more popular ones, there is Rosiglitazone (sold under the brand name Avandia, it reduces the insulin resistance of cells but its uptake has slowed significantly after suspected side effects such as heart failure became public), acarbose (which slows down the digestion and absorption of certain carbohydrates in the intestines), and gliptins (also known as DPP-4 inhibitors, they work by increasing insulin secretion and decreasing glucagon secretion in the pancreas).

No doubt, many other medicines with similar effects will appear in the future and they may, in many cases, also be incorporated into a dynamic blood glucose model.

Bibliography

[1] E. Ackerman, L. Gatewood, J. Rosevear, and G. D. Molnar, "Model studies of blood-glucose regulation," *The Bulletin of Mathematical Biophysics*, vol. 27, no. 1, pp. 21–37, 1965.

[2] F. Aguiree, A. Brown, N. Cho, G. Dahlquist, S. Dodd, T. Dunning, M. Hirst, C. Hwang, D. Magliano, C. Patterson, and C. Scott, "IDF diabetes atlas," 2013.

[3] Z. Al Helal, V. Rehbock, and R. Loxton, "Modelling and optimal control of blood glucose levels in the human body," *Journal of Industrial and Management Optimization*, vol. 11, no. 4, pp. 1149–1164, 2015.

[4] T. Alarcon, H. Byrne, and P. Maini, "A mathematical model of the effects of hypoxia on the cell-cycle of normal and cancer cells," *Journal of Theoretical Biology*, vol. 229, no. 3, pp. 395–411, 2004.

[5] S. Ali and R. Padhi, "Optimal blood glucose regulation of diabetic patients using single network adaptive critics," *Optimal Control Applications and Methods*, vol. 32, no. 2, pp. 196–214, 2011.

[6] H. Arabnia and Q. Tran, *Emerging Trends in Applications and Infrastructures for Computational Biology, Bioinformatics, and Systems Biology: Systems and Applications*. Morgan Kaufmann, 2016.

[7] C. Bailey and R. Turner, "Metformin," *The New England journal of medicine*, vol. 334, no. 9, p. 574, 1996.

[8] M. Berger and D. Rodbard, "Computer simulation of plasma insulin and glucose dynamics after subcutaneous insulin injection," *Diabetes Care*, vol. 12, no. 10, pp. 725–736, 1989.

[9] R. Bergman, "Pathogenesis and prediction of diabetes mellitus: lessons from integrative physiology," *The Mount Sinai Journal of Medicine, New York*, vol. 69, no. 5, pp. 280–290, 2002.

[10] R. Bergman, L. Phillips, and C. Cobelli, "Physiologic evaluation of factors controlling glucose tolerance in man: measurement of insulin sensitivity and beta-cell glucose

sensitivity from the response to intravenous glucose." *Journal of Clinical Investigation*, vol. 68, no. 6, pp. 1456–1467, 1981.

[11] M. Breton, "Physical activitythe major unaccounted impediment to closed loop control," *Journal of diabetes science and technology*, vol. 2, no. 1, pp. 169–174, 2008.

[12] F. Chee and T. Fernando, *Closed-loop control of blood glucose: Lecture Notes in Control and Information Sciences*. Berlin: Springer, 2007.

[13] C. Cobelli, G. Federspil, G. Pacini, A. Salvan, and C. Scandellari, "An integrated mathematical model of the dynamics of blood glucose and its hormonal control," *Mathematical Biosciences*, vol. 58, no. 1, pp. 27–60, 1982.

[14] F. Curtis and M. Overton, "A sequential quadratic programming algorithm for nonconvex, nonsmooth constrained optimization," *Society for Industrial and Applied Mathematics Journal on Optimization*, vol. 22, no. 2, pp. 474–500, 2012.

[15] C. Dalla Man, D. Raimondo, R. Rizza, and C. Cobelli, "GIM, simulation software of meal glucoseinsulin model," *Journal of Diabetes Science and Technology*, vol. 1, no. 3, pp. 323–330, 2007.

[16] M. Derouich and A. Boutayeb, "The effect of physical exercise on the dynamics of glucose and insulin," *Journal of biomechanics*, vol. 35, no. 7, pp. 911–917, 2002.

[17] M. Fisher, "A semiclosed-loop algorithm for the control of blood glucose levels in diabetics," *Biomedical Engineering, IEEE Transactions on*, vol. 38, no. 1, pp. 57–61, 1991.

[18] M. Fisher and K. Teo, "Optimal insulin infusion resulting from a mathematical model of blood glucose dynamics," *Biomedical Engineering, IEEE Transactions on*, vol. 36, no. 4, pp. 479–486, 1989.

[19] M. Fowler, "Microvascular and macrovascular complications of diabetes ," *Clinical Diabetes*, vol. 26, no. 2, p. 7782, 2008.

[20] L. Fridlyand and L. Philipson, "Glucose sensing in the pancreatic beta cell: A computational systems analysis," *Theoretical Biology and Medical Modelling*, vol. 7, 2010.

[21] C. Goh and K. Teo, "MISER: a FORTRAN program for solving optimal control problems ," *Advances in Engineering Software*, vol. 28, 1988.

[22] M. Hernández-Ordoñez and D. Campos-Delgado, "An extension to the compartmental model of type 1 diabetic patients to reproduce exercise periods with glycogen

depletion and replenishment," *Journal of Biomechanics*, vol. 41, no. 4, pp. 744–752, 2008.

[23] R. Hovorka, V. Canonico, L. Chassin, U. Haueter, M. Massi-Benedetti, M. Federici, T. Pieber, H. Schaller, L. Schaupp, T. Vering, and M. Wilinska, "Nonlinear model predictive control of glucose concentration in subjects with type 1 diabetes," *Physiological measurement*, vol. 25, no. 4, p. 905, 2004.

[24] L. Jennings, M. Fisher, K. Teo, and C. Goh, " MISER3: solving optimal control problemsan update ," *Advances in Engineering Software and Workstations*, vol. 13, no. 4, pp. 190–196, 1991.

[25] ——, *MISER3 Optimal Control Software: Theory and User Manual*, The University of Western Australia, Perth, July 2004.

[26] T. Kobayashi, S. Sawano, T. Itoh, K. Kosaka, H. Hirayama, and Y. Kasuya, "The pharmacokinetics of insulin after continuous subcutaneous infusion or bolus subcutaneous injection in diabetic patients," *Diabetes*, vol. 32, no. 4, pp. 331–336, 1983.

[27] M. Korach-André, H. Roth, D. Barnoud, M. Péan, F. Péronnet, and X. Leverve, "Glucose appearance in the peripheral circulation and liver glucose output in men after a large 13C starch meal," *The American journal of clinical nutrition*, vol. 80, no. 4, pp. 881–886, 2004.

[28] L. Kovács, B. Kulcsar, A. György, and Z. Benyó, "Robust servo control of a novel type 1 diabetic model," *Optimal Control Applications and Methods*, vol. 32, no. 2, pp. 215–238, 2011.

[29] H. Lee, K. Teo, V. Rehbock, and L. Jennings, "Control parametrization enhancing technique for optimal discrete-valued control problems," *Automatica*, vol. 35, no. 8, pp. 1401–1407, 1999.

[30] Q. Lin, R. Loxton, and K. Teo, "The control parameterization method for nonlinear optimal control: a survey," *Journal of Industrial and Management Optimization*, vol. 10, no. 1, pp. 275–309, 2014.

[31] W. Liu and F. Tang, "Modeling a simplified regulatory system of blood glucose at molecular levels," *Journal of Theoretical Biology*, vol. 252, no. 4, pp. 608–620, 2008.

[32] R. Loxton, Q. Lin, V. Rehbock, and K. Teo, "Control parameterization for optimal control problems with continuous inequality constraints: New convergence results," *Numerical Algebra, Control and Optimization*, vol. 2, no. 3, pp. 571–599, 2012.

[33] R. Loxton, K. Teo, and V. Rehbock, "Robust suboptimal control of nonlinear systems," *Applied Mathematics and Computation*, vol. 217, no. 14, pp. 6566–6576, 2011.

[34] ——, "Optimal control problems with multiple characteristic time points in the objective and constraints," *Automatica*, vol. 44, no. 11, pp. 2923–2929, 2008.

[35] D. Luenberger and Y. Ye, *Linear and Nonlinear Programming*, 3rd ed. New York: Springer, 2008.

[36] S. Lynch and B. Bequette, "Model predictive control of blood glucose in type I diabetics using subcutaneous glucose measurements," in *Proceedings of the American Control Conference, Anchorage, AK*, pp. 4039–4043.

[37] C. Man, R. Rizza, and C. Cobelli, "Meal simulation model of the glucose-insulin system," *Biomedical Engineering, IEEE Transactions on*, vol. 54, no. 10, pp. 1740–1749, 2007.

[38] G. Marchetti, M. Barolo, L. Jovanovi, H. Zisser, and D. Seborg, "An Improved PID Switching Control Strategy for Type 1 Diabetes," in *the 28th IEEE EMBS Annual International Conference, New York*.

[39] M. Markakis, G. Mitsis, G. Papavassilopoulos, P. Ioannou, and V. Marmarelis, "A switching control strategy for the attenuation of blood glucose disturbances," *Optimal Control Applications and Methods*, vol. 32, no. 2, pp. 185–195, 2011.

[40] R. Martin, K. Teo, and M. D'Incalci, *Optimal control of drug administration in cancer chemotherapy*. World Scientific, 1994.

[41] R. Martin, "Optimal control drug scheduling of cancer chemotherapy," *Automatica*, vol. 28, no. 6, pp. 1113–1123, 1992.

[42] R. Muñoz-Tamayo, F. Mairet, and O. Bernard, "Optimizing microalgal production in raceway systems," *Biotechnology Progress*, vol. 29, no. 2, pp. 543–552, 2013.

[43] J. Nocedal and S. Wright, *Numerical optimization*. New York: Springer Science and Business Media, 2006.

[44] G. Nucci and C. Cobelli, "Models of subcutaneous insulin kinetics. A critical review," *Computer Methods and Programs in Biomedicine*, vol. 62, no. 3, pp. 249–257, 2000.

[45] K. Palmer and R. Brogden, "Gliclazide," *Drugs*, vol. 46, no. 1, pp. 92–125, 1993.

[46] R. Parker, F. Doyle III, and N. Peppas, "A model-based algorithm for blood glucose control in type I diabetic patients," *Biomedical Engineering, IEEE Transactions on*, vol. 46, no. 2, pp. 148–157, 1999.

[47] G. Quiroz, C. Flores-Gutiérrez, and R. Femat, "Suboptimal $H\infty$ hyperglycemia control on T1DM accounting biosignals of exercise and nocturnal hypoglycemia," *Optimal Control Applications and Methods*, vol. 32, no. 2, pp. 239–252, 2011.

[48] A. Rao, "A survey of numerical methods for optimal control," in *AAS/AIAA Astrodynamics specialist conference AAS Paper 09334 , Pittsburgh, PA*, 2009, p. AAS Paper 09334.

[49] A. Roy and R. S. Parker, "A phenomenological model of plasma FFA, glucose, and insulin concentrations during rest and exercise," in *American Control Conference (ACC), 2010*, June 2010, pp. 5161–5166.

[50] K. Schittkowski, "A robust implementation of a sequential quadratic programming algorithm with successive error restoration," *Optimization Letters*, vol. 5, no. 2, pp. 283–296, 2011.

[51] K. Schittkowski and Y. Yuan, "Sequential quadratic programming methods," *Wiley Encyclopedia of Operations Research and Management Science*, 2011.

[52] A. Sieg, R. H. Guy, and M. B. Delgado-Charro, "Noninvasive and minimally invasive methods for transdermal glucose monitoring ," *Diabetes Technology and Therapeutics*, vol. 7, no. 1, p. 174197, 2005.

[53] J. Sorensen, "A physiologic model of glucose metabolism in man and its use to design and assess improved insulin therapies for diabetes," Ph.D. dissertation, Chemical Engineering Department, Massachusetts Institute of Technology, 1985.

[54] K. Teo and C. Goh, "A simple computational procedure for optimization problems with functional inequality constraints," *IEEE Transactions on Automatic Control*, vol. 32, no. 10, pp. 940–941, 1987.

[55] K. Teo, C. Goh, and K. Wong, *A Unified Computational Approach to Optimal Control Problems*. Longman Scientific and Technical, Essex, 1991.

[56] K. Teo and L. Jennings, "Nonlinear optimal control problems with continuous state inequality constraints," *Journal of Optimization Theory and Applications*, vol. 63, no. 1, pp. 1–22, 1989.

[57] Z. Trajanoski, P. Wach, P. Kotanko, A. Ott, and F. Skraba, "Pharmacokinetic model for the absorption of subcutaneously injected soluble insulin and monomeric insulin analogues," *Biomedizinische Technik. Biomedical Engineering*, vol. 38, no. 9, pp. 224–231, 1993.

Every reasonable effort has been made to acknowledge the owners of copyright material. I would be pleased to hear from any copyright owner who has been omitted or incorrectly acknowledged.